Electronic Supplementary Information for Chemical Communications

Self-assembly of *pseudo*-rotaxane and rotaxane complexes using an electrostatic slippage approach

Aldo C. Catalán and Jorge Tiburcio*

Departamento de Química
Centro de Investigación y de Estudios Avanzados (Cinvestav)
Avenida IPN 2508, Colonia Zacatenco, 07360, Ciudad de México, México.
Tel: +52 5557473721
E-mail:jtiburcio@cinvestav.mx

Table of Contents

1. General

All chemicals were purchased from Aldrich and used without further purification. NMR spectra were recorded on a Bruker AVANCE 300 MHz, Jeol Eclipse 400 MHz or Jeol ECA 500 MHz spectrometers, locked to the deuterated solvent. Mass spectra were obtained on an Agilent G1969A electrospray-ionization time-of-flight spectrometer. Single-crystal X-ray diffraction was performed in an Enraf–Nonius Kappa diffractometer fitted with a CCD based detector using MoK_α radiation (0.71073 Å). Diffraction data and unit-cell parameters were consistent with the assigned space group. The structure was solved by direct methods, completed by subsequent Fourier syntheses and refined with full-matrix least-squares methods against $|F^2|$ data. All non-hydrogen atoms were refined anisotropically. All hydrogen atoms were treated as idealized contributions. Scattering factors and anomalous dispersion coefficients are contained in the SHELXTL 5.03 program library. Ball-and-stick diagrams were prepared using DIAMOND 3.3. Sample temperature for the rate constant determinations was controlled with a PolyScience circulating bath and NMR equipment controller. Linear curve fitting of the van't Hoff plots was done using Microsoft Office Excel 2007. Non-linear curve fitting of the plots for the rate constants determinations was achieved utilizing OriginPro 8.0.

2. Synthesis and characterisation

Synthesis of the dumbbell precursor **INF**. The dumbbell precursor **INF** was synthesised modifying a previously reported procedure,[1] as depicted in Scheme S2.1.

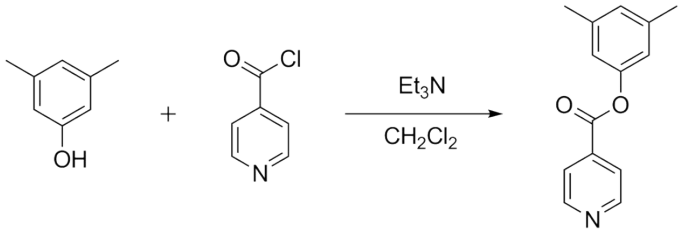

Scheme S2.1. Synthesis of the 3,5-dimethylphenyl isonicotinate (**INF**).

To a solution containing 0.67g of 3,5-dimethylphenol (5.34mmol) in CH_2Cl_2 (8mL) was added 1.00g of isonicotinoyl chloride hydrochloride (5.34mmol). Just after mixing, 3mL of triethylamine (21.3mmol) dissolved in CH_2Cl_2 (8mL) was added drop wise. The mixture was refluxed for 1 day. The solid was separated by filtration and the filtrate was washed repeatedly with water. After the organic layer had dried (Na_2SO_4 anhydrous), the solvent was evaporated, leaving an oil, which crystallized as a white solid (1.12g, 90%). The 3,5-dimethylphenyl isonicotinate (**INF**) was utilized for the synthesis of the dumbbells without further purification.

Synthesis of [**1-Pi·H**][PF_6]$_2$. The 1-(2-bromoethyl)piperidinium bromide was synthesised according to a previously reported procedure,[2] as depicted in Scheme S2.2 (2.98g, 73%).

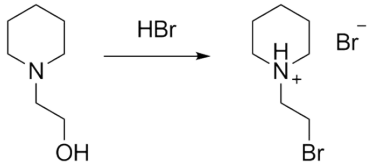

Scheme S2.2. Synthesis of the 1-(2-bromoethyl)piperidinium bromide.

Isonicotinate **INF** (1.07g, 4.71mmol), 1-(2-bromoethyl)piperidinium bromide (0.27g, 0.99mmol) and CH_3CN (5mL) were refluxed for 5 days. The pale yellow solid was filtered and washed with $CHCl_3$ (0.38g, 77%). The dumbbell as the bromide salt could be transformed into the hexafluorophosphate salt by anion exchange in the presence of 1 equivalent of HBr (0.35g, 73%). ^{1}H NMR (300 MHz, CD_3NO_2) δ_H 9.11 (2H, d, J = 6.4 Hz, H_f), 8.78 (2H, d, J = 6.4 Hz, H_g), 7.04 (1H, s, H_j), 6.94 (2H, s, H_h), 5.30 (2H, t, J = 8.1 Hz, H_e), 3.99 (2H, t, J = 8.0 Hz, H_d), 3.84-3.28 (4H, m, H_c), 2.34 (6H, s, H_i), 2.07-1.62 (6H, br.m, H_b and H_a). ^{13}C NMR (75 MHz, CD_3NO_2) δ_C 160.75 ($C_{carbonyl}$); 150.26 (C_{ipso}); 146.58 (C_f); 146.19 (C_{ipso}); 140.27 (C_{ipso}); 128.86 (C_g); 128.42 (C_j); 118.38 (C_h); 55.64 (C_c); 55.53 (C_e); 55.18 (C_d); 22.98 (C_b); 20.65 (C_a); 19.85 (C_i). ESI-HRMS: *m*/*z* found for [**1-Pi·H**]$^{2+}$ 170.107540, calculated 170.106990, error 3.229546ppm; *m*/*z* found for [**1-Pi**]$^{1+}$ 339.206461, calculated 339.206704, error -0.718723ppm.

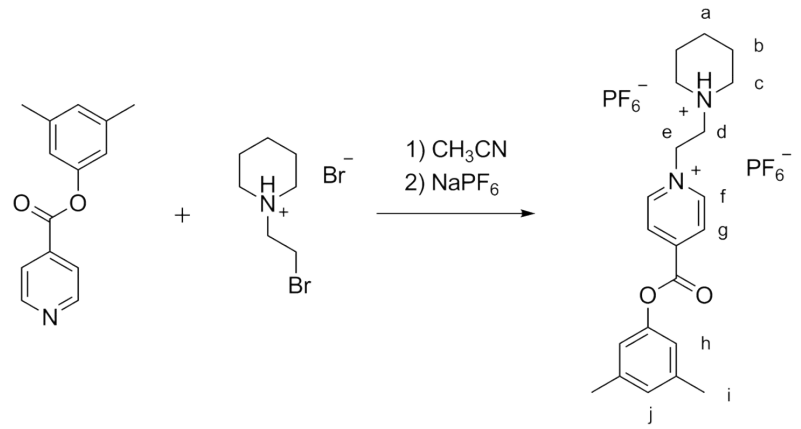

Scheme S2.3. Synthesis of the dumbbell [**1-Pi·H**][PF_6]$_2$.

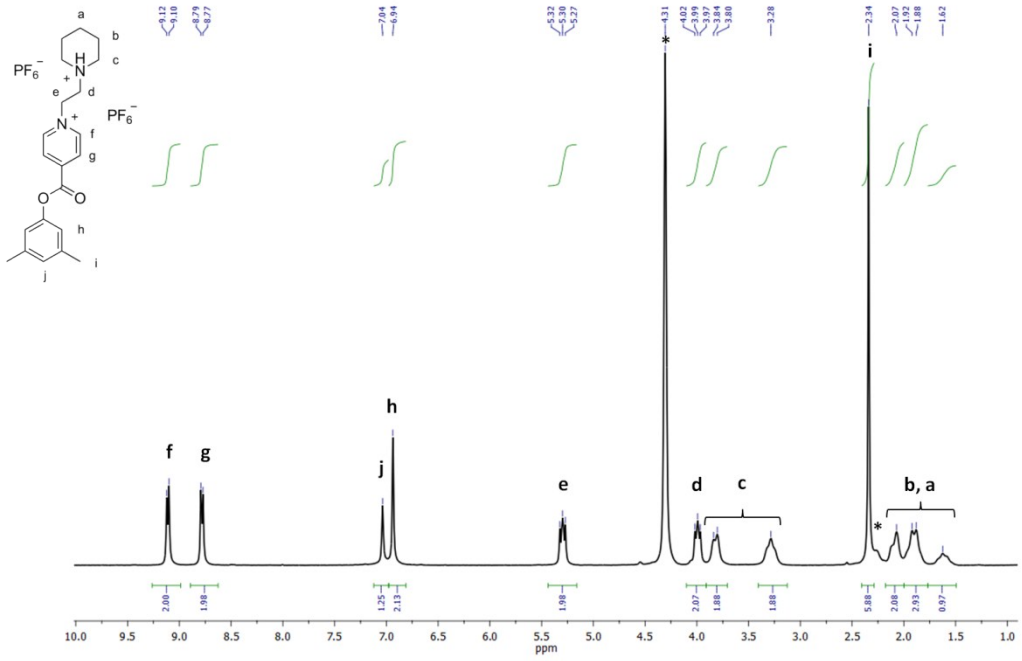

Figure S2.1. Assigned ^{1}H NMR spectrum of the dumbbell [**1-Pi·H**][PF_6]$_2$ (300MHz, CD_3NO_2, rt, * = residual solvents).

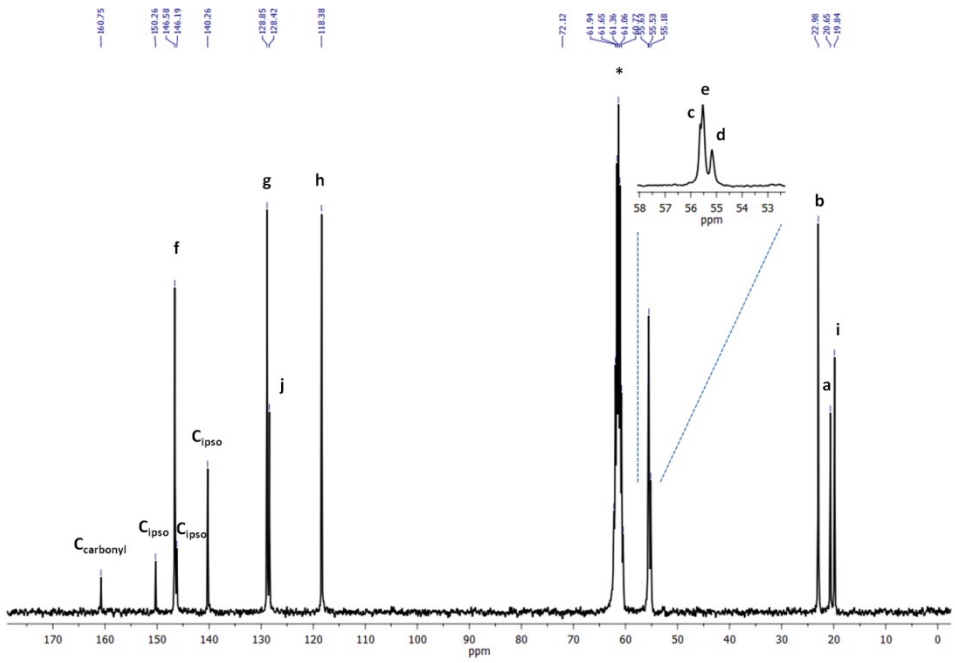

Figure S2.2. Assigned ^{13}C NMR spectrum of the dumbbell [**1-Pi·H**][PF_6]$_2$ (75MHz, CD_3NO_2, rt, * = residual solvent).

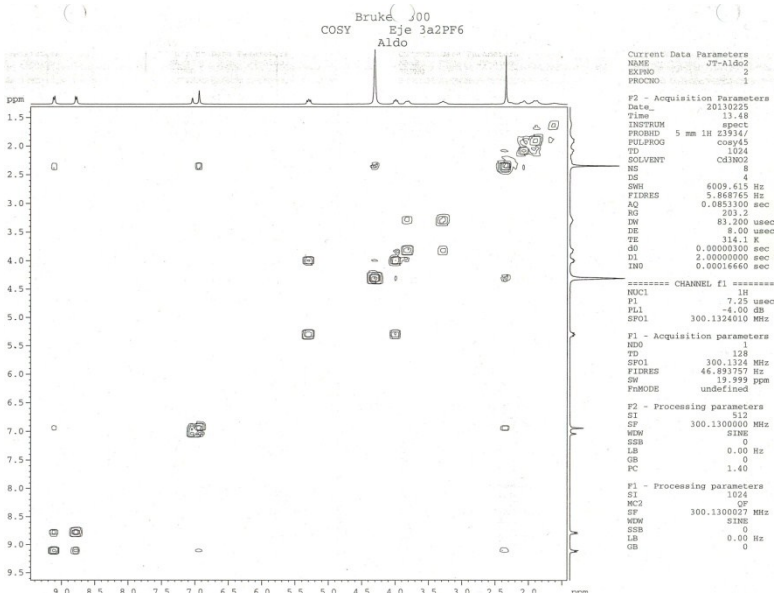

Figure S2.3. 2D NMR COSY of the dumbbell [**1-Pi·H**][PF_6]$_2$ (300MHz, CD_3NO_2, rt).

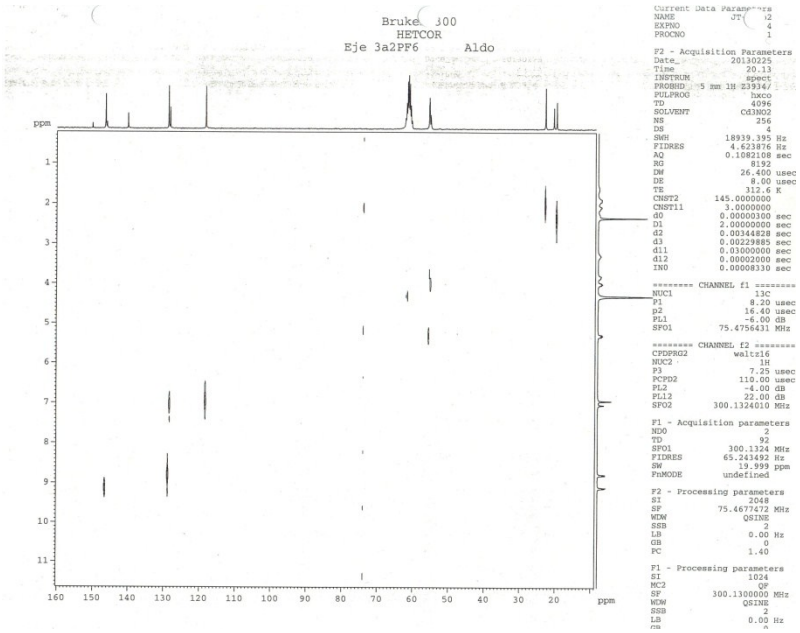

Figure S2.4. 2D NMR HETCOR of the dumbbell [**1-Pi·H**][PF_6]$_2$ (CD_3NO_2, rt).

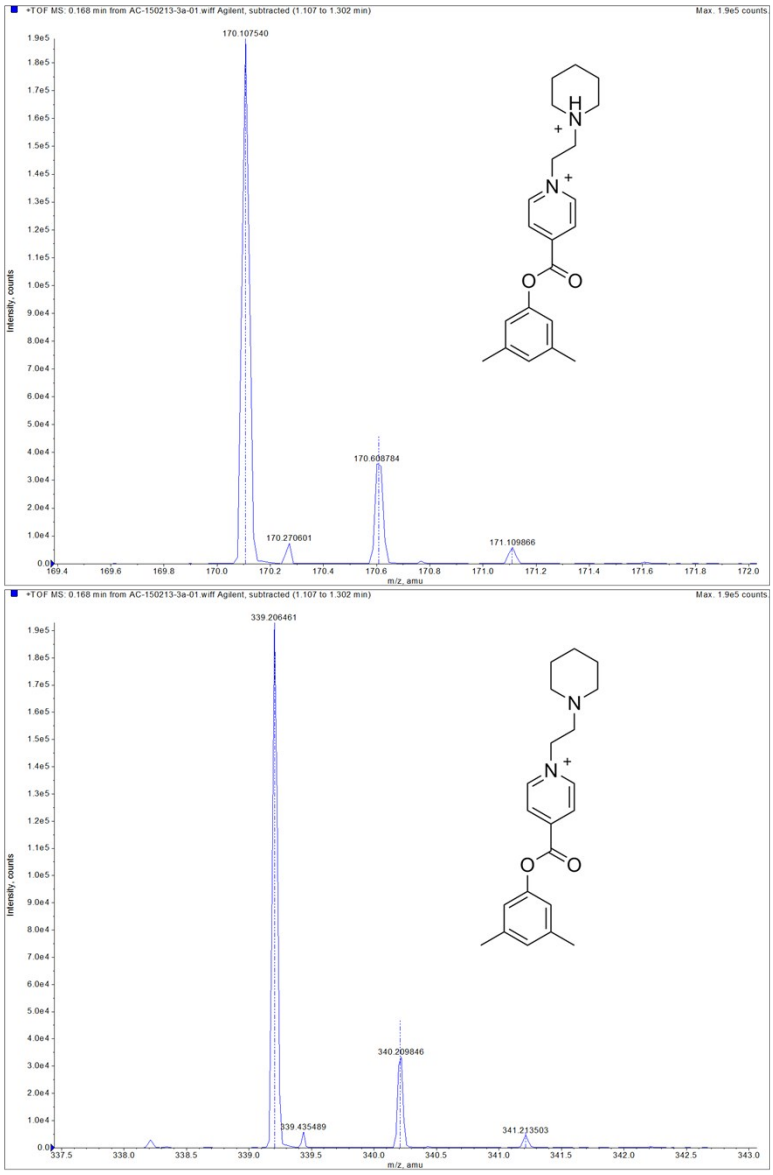

Figure S2.5. ESI-HRMS spectra of [**1-Pi·H**][PF_6]$_2$. Experimental molecular ion (continous line) and calculated isotopic profile (broken line).

Synthesis of [**1-Mp·H**][PF_6]$_2$. The 4-(2-bromoethyl)morpholin-4-ium bromide was synthesised from 2-morpholinoethanol,[2] as depicted in Scheme S2.4 (3.63g, 81%).

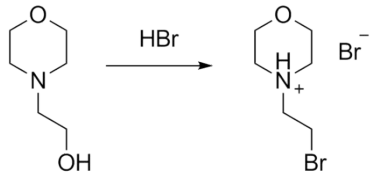

Scheme S2.4. Synthesis of the 4-(2-bromoethyl)morpholin-4-ium bromide.

Isonicotinate **INF** (0.50g, 2.20mmol), 4-(2-bromoethyl)morpholin-4-ium bromide (0.12g, 0.44mmol) and CH_3CN (5mL) were refluxed for 5 days. The white solid was filtered and washed with $CHCl_3$ (0.16g, 74%). The bromide salt obtained can be transformed into the corresponding hexafluorophosphate salt by anion exchange in the presence of 1 equivalent of HBr (0.16g, 78 %). ^{1}H NMR (400 MHz, CD_3NO_2) δ_H 9.21 (2H, d, J = 6.8 Hz, H_e), 8.79 (2H, d, J = 6.8 Hz, H_f), 7.06 (1H, s, H_i), 6.96 (2H, s, H_g), 5.37 (2H, t, J = 7.2 Hz, H_d), 4.05 (4H, br.s, H_b), 3.94 (2H, t, J = 7.2 Hz, H_c), 3.48 (4H, br.s, H_a), 2.36 (6H, s, H_h). ^{13}C NMR (100 MHz, CD_3NO_2) δ_C 160.95 ($C_{carbonyl}$); 150.39 (C_{ipso}); 146.73 (C_e); 146.11 (C_{ipso}); 140.38 (C_{ipso}); 128.81 (C_f); 128.53 (C_i); 118.52 (C_g); 63.85 (C_a); 55.59 (C_c and C_d); 53.28 (C_b); 19.98 (C_h). ESI-HRMS: *m/z* found for [**1-Mp·H**]$^{2+}$ 171.097773, calculated 171.096622, error 6.721819ppm; *m/z* found for [**1-Mp**]$^{1+}$ 341.186143, calculated 341.185969, error 0.508941ppm.

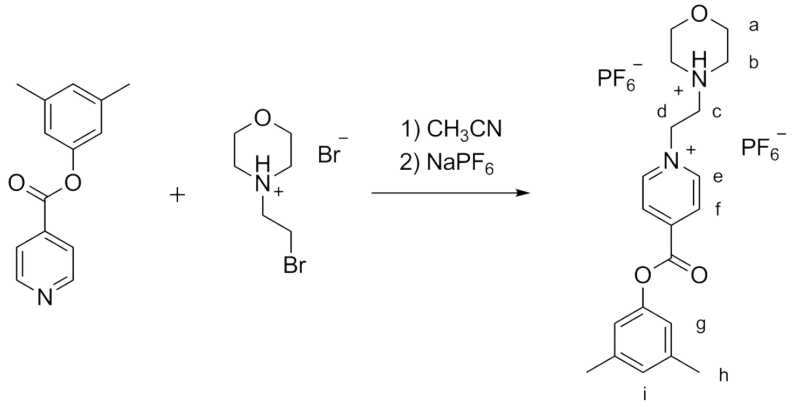

Scheme S2.5. Synthesis of the dumbbell [**1-Mp·H**][PF_6]$_2$.

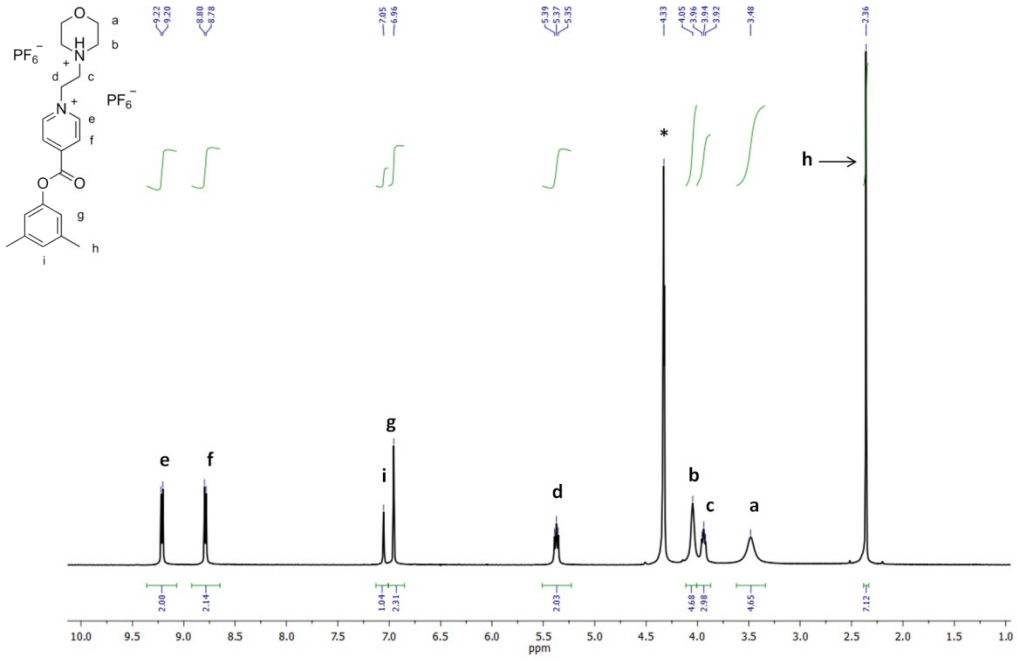

Figure S2.6. Assigned ^{1}H NMR spectrum of the dumbbell [**1-Mp·H**][PF_6]$_2$ (400MHz, CD_3NO_2, rt, * = residual solvent).

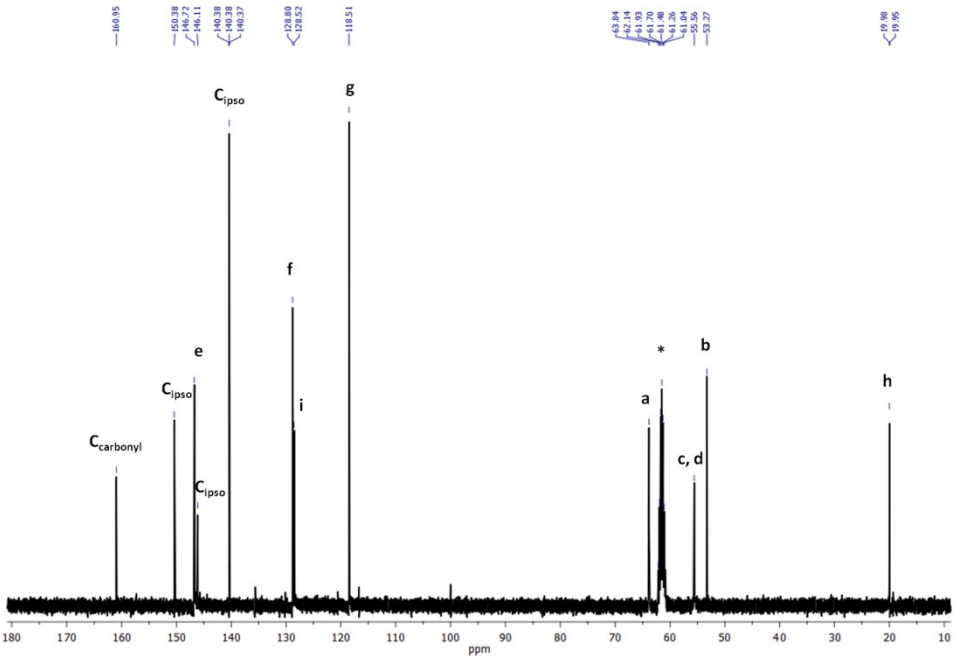

Figure S2.7. Assigned ^{13}C NMR spectrum of the dumbbell [**1-Mp·H**][PF_6]$_2$ (100MHz, CD_3NO_2, rt, * = residual solvent).

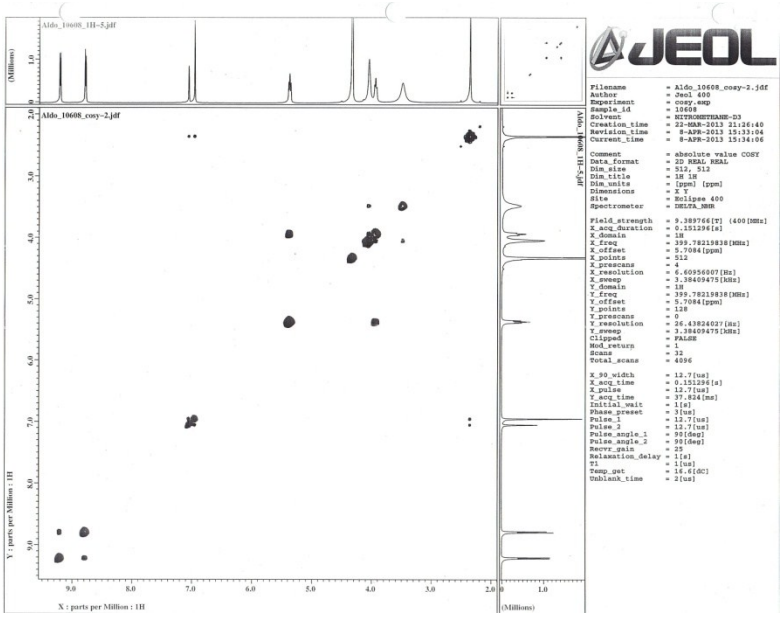

Figure S2.8. 2D NMR COSY of the dumbbell [**1-Mp·H**][PF_6]$_2$ (400MHz, CD_3NO_2, rt).

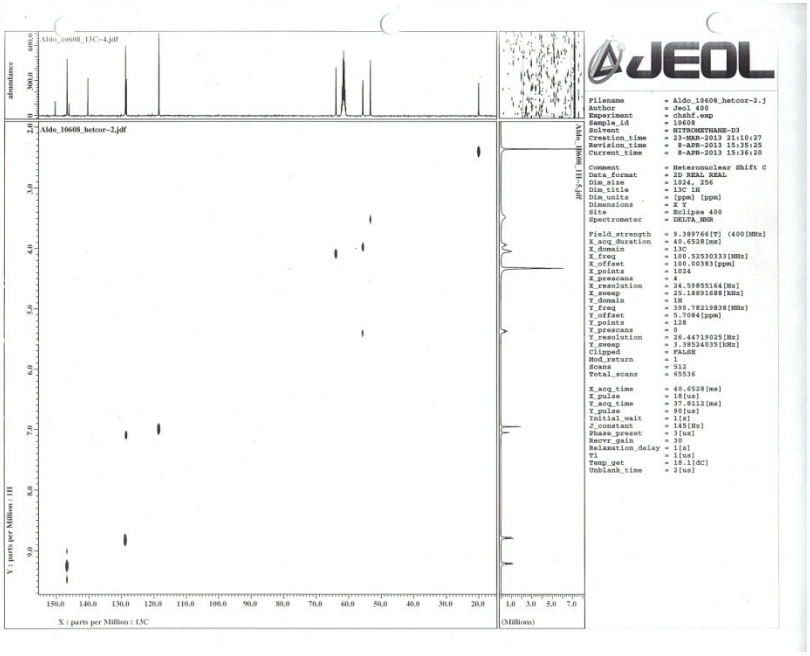

Figure S2.9. 2D NMR HETCOR of the dumbbell [**1-Mp**·**H**][PF_6]$_2$ (CD_3NO_2, rt).

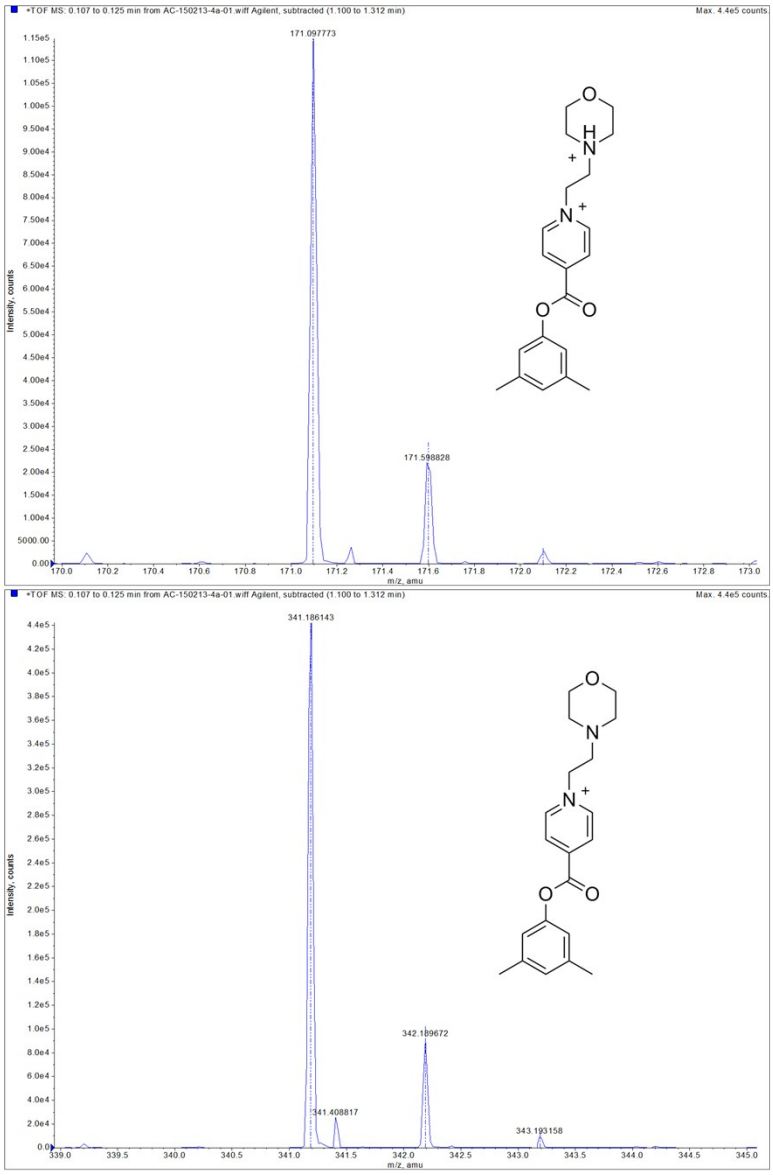

Figure S2.10. ESI-HRMS spectra of [**1-Mp·H**][PF_6]$_2$. Experimental molecular ion (continous line) and calculated isotopic profile (broken line).

Synthesis of [**1-Tm·H**][PF_6]$_2$. The 4-(2-hydroxyethyl)thiomorpholin-4-ium bromide was synthesised modifying a previous reported procedure,[3] as depicted in Scheme S2.6. Thiomorpholine (1.40mL, 13.64mmol), 2-bromoethanol (1.02mL, 13.64mmol) and CH_3CN (6mL) were refluxed for 1 day. The white solid was filtered and washed with cold $(CH_3)_2CO$ (1.79g, 57%). The 4-(2-hydroxyethyl)thiomorpholin-4-ium bromide was deprotonated with three equivalents of Et_3N in CH_2Cl_2, the excess of base and the triethylammonium bromide were removed washing the organic layer with plenty water; after the organic layer had dried (Na_2SO_4 anhydrous), the solvent was evaporated, leaving the 2-thiomorpholinoethanol as a colourless oil (0.54g, 47%). To a THF solution (10mL) of 2-thiomorpholinoethanol (0.25g, 1.71mmol) and CBr_4 (1.14g, 3.42mmol) was added a THF solution (4mL) of PPh_3 (0.90g, 3.42mmol) dropwise at 0 °C. The reaction mixture was allowed to warm slowly to room temperature, stirred for an additional 18 hours. The solid was

filtered and washed with cold EtOH, yielding the 4-(2-bromoethyl)thiomorpholine as a white solid (0.25g, 68%).

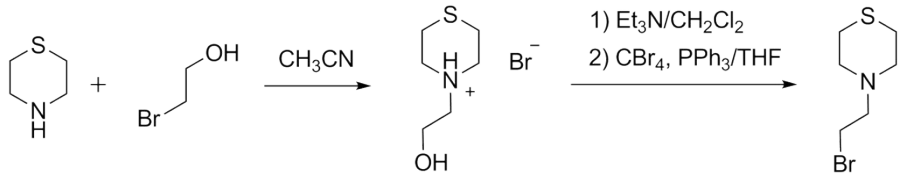

Scheme S2.6. Synthesis of the 4-(2-bromoethyl)thiomorpholine.

Isonicotinate **INF** (0.50g, 2.20mmol), 4-(2-bromoethyl)thiomorpholine (0.15g, 0.73mmol) and CH_3CN (5mL) were refluxed for 5 days. The pale yellow solid was filtered and washed with CH_2Cl_2 (0.23g, 71%). The dumbbell as the bromide salt could be transformed into the hexafluorophosphate salt by anion exchange in the presence of 1 equivalent of HBr (0.25g, 87%). ^{1}H NMR (300 MHz, CD_3NO_2) δ_H 9.13 (2H, d, J = 6.4 Hz, H_e), 8.78 (2H, d, J = 6.3 Hz, H_f), 7.04 (1H, s, H_i), 6.94 (2H, s, H_g), 5.32 (2H, t, J = 7.7 Hz, H_d), 4.02 (2H, t, J = 7.8 Hz, H_c), 4.02-3.56 (4H, br.m, H_b), 3.18-3.03 (4H, br.m, H_a), 2.34 (6H, s, H_h). ^{13}C NMR (75 MHz, CD_3NO_2) δ_C 160.78 ($C_{carbonyl}$); 150.25 (C_{ipso}); 146.64 (C_e); 146.19 (C_{ipso}); 140.28 (C_{ipso}); 128.84 (C_f); 128.43 (C_i); 118.39 (C_g); 55.93 (C_b); 55.71 (C_d); 55.36 (C_c); 24.68 (C_a); 19.86 (C_h). ESI-HRMS: *m*/*z* found for [**1-Tm**·**H**]$^{2+}$ 179.086337, calculated 179.085201, error 6.340564ppm; *m*/*z* found for [**1-Tm**]$^{1+}$ 357.163700, calculated 357.163126, error 1.605659ppm.

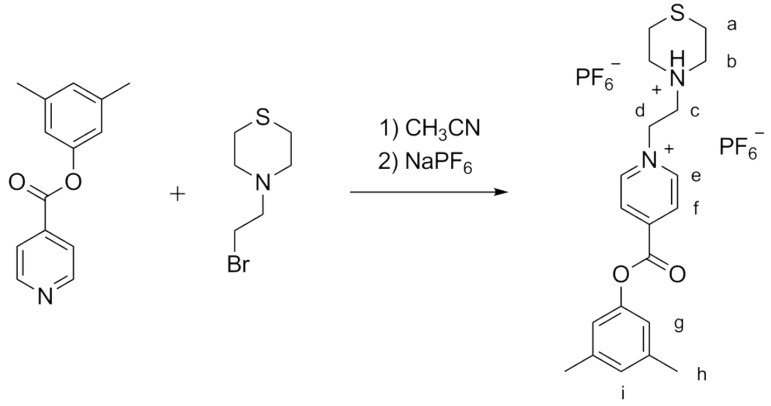

Scheme S2.7. Synthesis of the dumbbell [**1-Tm**·**H**][PF_6]$_2$.

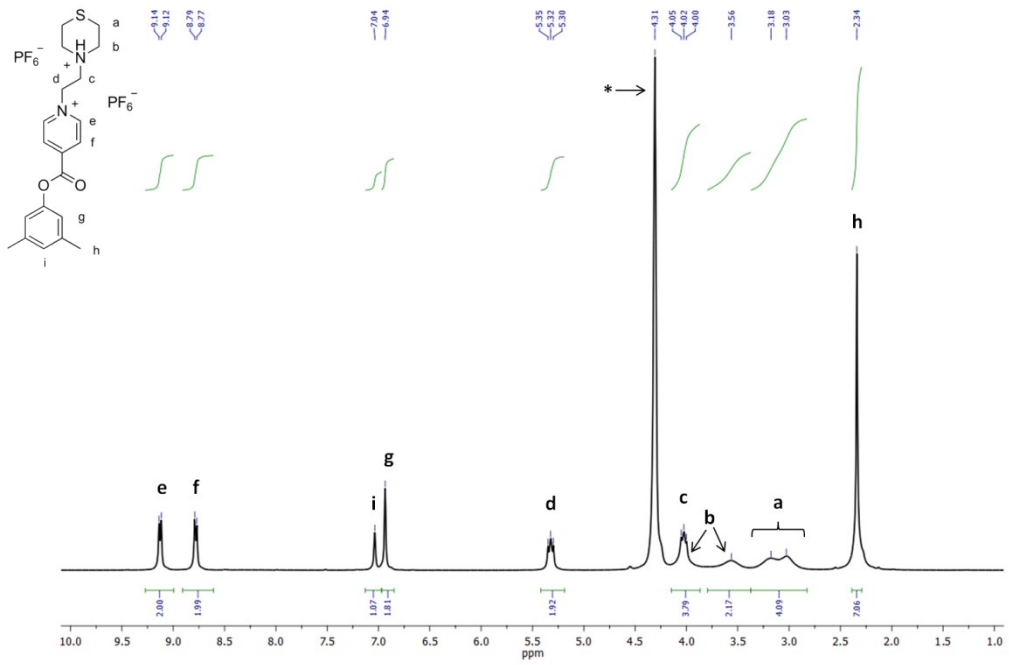

Figure S2.11. Assigned ^{1}H NMR spectrum of the dumbbell [**1-Tm·H**][PF_6]$_2$ (300MHz, CD_3NO_2, rt, * = residual solvent).

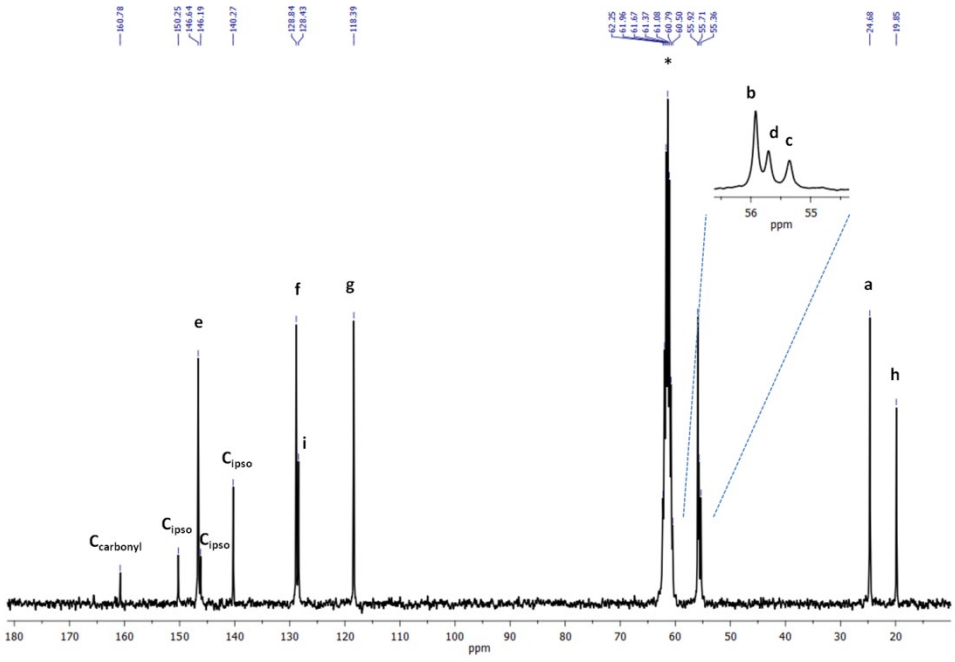

Figure S2.12. Assigned ^{13}C NMR spectrum of the dumbbell [**1-Tm·H**][PF_6]$_2$ (75MHz, CD_3NO_2, rt, * = residual solvent).

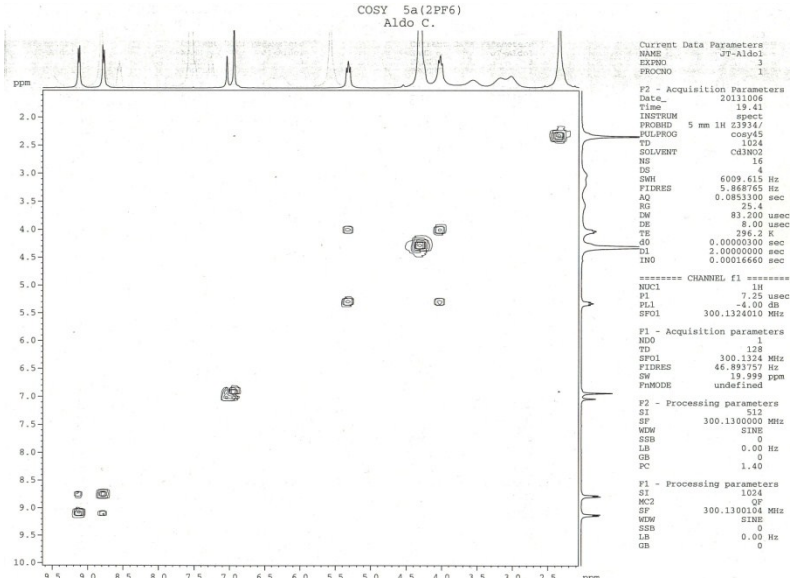

Figure S2.13. 2D NMR COSY of the dumbbell [**1-Tm·H**][PF_6]$_2$ (300MHz, CD_3NO_2, rt).

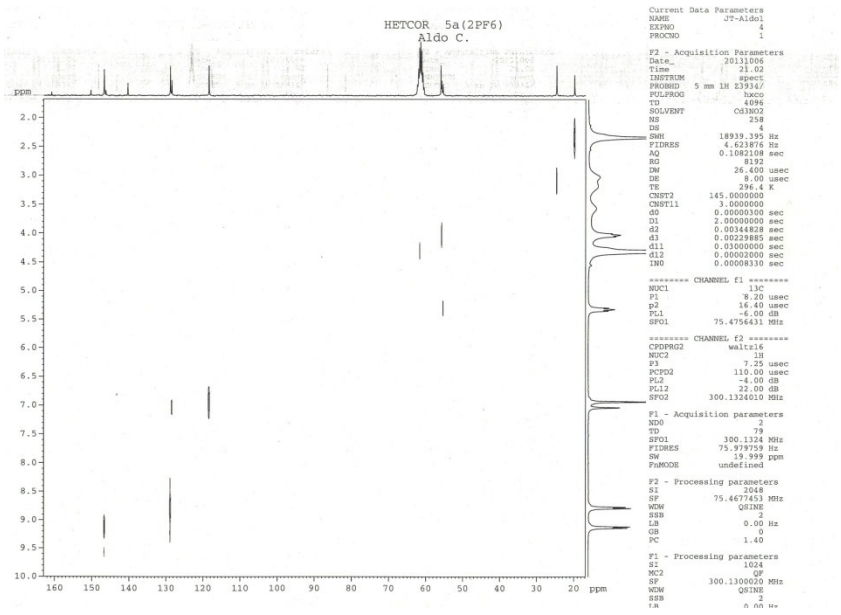

Figure S2.14. 2D NMR HETCOR of the dumbbell [**1-Tm·H**][PF_6]$_2$ (CD_3NO_2, rt).

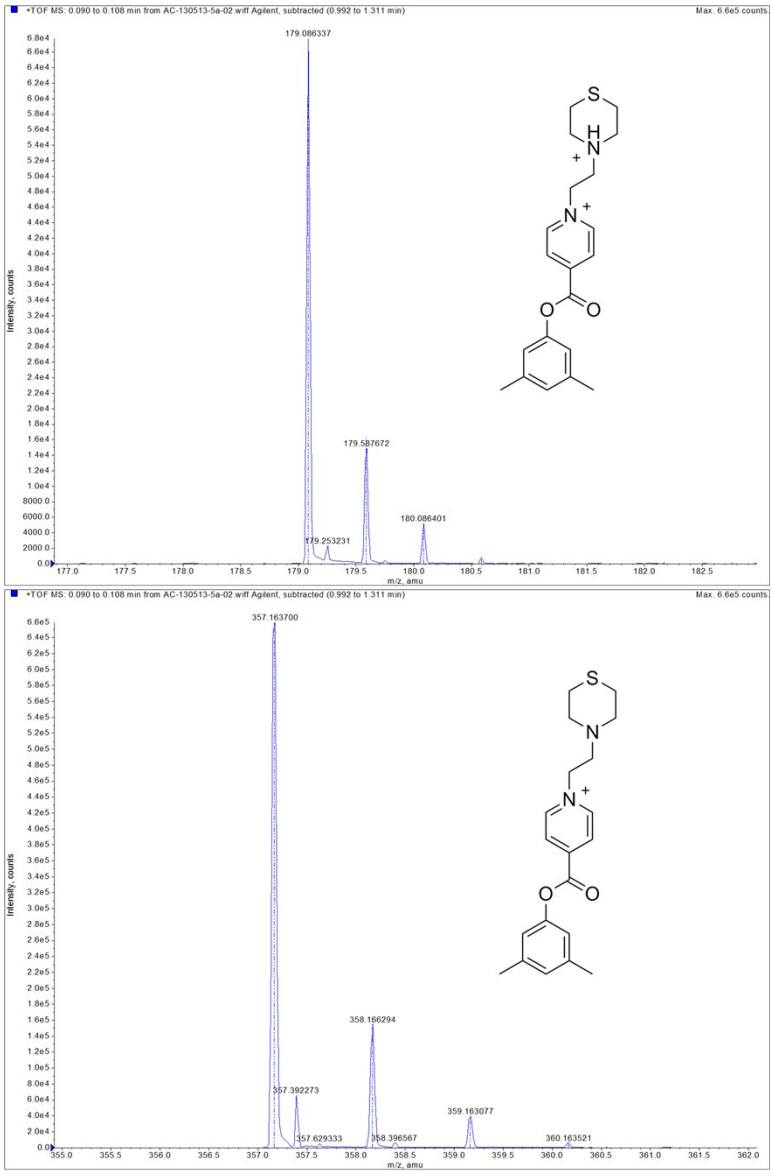

Figure S2.15. ESI-HRMS spectra of [**1-Tm·H**][PF_6]$_2$. Experimental molecular ion (continous line) and calculated isotopic profile (broken line).

Synthesis of [**1-Aze·H**][PF_6]$_2$. The 1-(2-hydroxyethyl)azepanium bromide was synthesised modifying a previous reported procedure,[4] as depicted in Scheme S2.8. Azepane (1mL, 8.78mmol), 2-bromoethanol (1.5mL, 20.10mmol) and CH_3CN (5mL) were refluxed for 36 hours. An excess of diethyl ether was added to the reaction flask and the precipitated white crystalline solid was filtered and washed with cold $(CH_3)_2CO$ (1.54g, 78%). The 1-(2-bromoethyl)azepanium bromide was synthesised from the 1-(2-hydroxyethyl)azepanium bromide based on the same methodology (0.82g, 36%).[2]

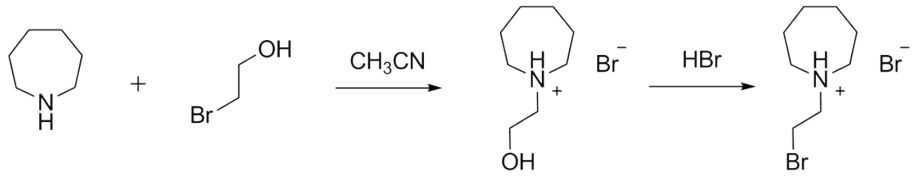

Scheme S2.8. Synthesis of 1-(2-bromoethyl)azepanium bromide.

Isonicotinate **INF** (1.08g, 4.75mmol), 1-(2-bromoethyl)azepanium bromide (0.26g, 0.91mmol) and CH_3CN (5mL) were refluxed for 3 days. The pale yellow solid was filtered and washed with $CHCl_3$ (0.30g, 64%). The bromide salt can be easily transformed into the hexafluorophosphate salt by anion exchange in the presence of 1 equivalent of HBr (0.27g, 72%). ^{1}H NMR (300 MHz, CD_3NO_2) δ_H 9.12 (2H, d, J = 6.1 Hz, H_g), 8.78 (2H, d, J = 6.0 Hz, H_h), 7.41 (1H, br.s, H_c), 7.04 (1H, s, H_k), 6.94 (2H, s, H_i), 5.30 (2H, t, J = 7.8 Hz, H_f), 4.05 (2H, br.s, H_e), 3.80-3.51 (4H, br.m, H_d), 2.34 (6H, s, H_j), 2.06 (4H, br.m, H_b), 1.79 (4H, br.s, H_a). ^{13}C NMR (75 MHz, CD_3NO_2) δ_C 160.77 ($C_{carbonyl}$); 150.25 (C_{ipso}); 146.60 (C_g); 146.12 (C_{ipso}); 140.27 (C_{ipso}); 128.86 (C_h); 128.43 (C_k); 118.39 (C_i); 57.12 (C_d); 55.95 (C_f); 55.61 (C_e); 25.76 (C_a); 23.47 (C_b); 19.85 (C_j). ESI-HRMS: *m*/*z* found for [**1-Aze·H**]$^{2+}$ 177.115589, calculated 177.114815, error 4.366242ppm; *m*/*z* found for [**1-Aze**]$^{1+}$ 353.222189, calculated 353.222354, error -0.469607ppm.

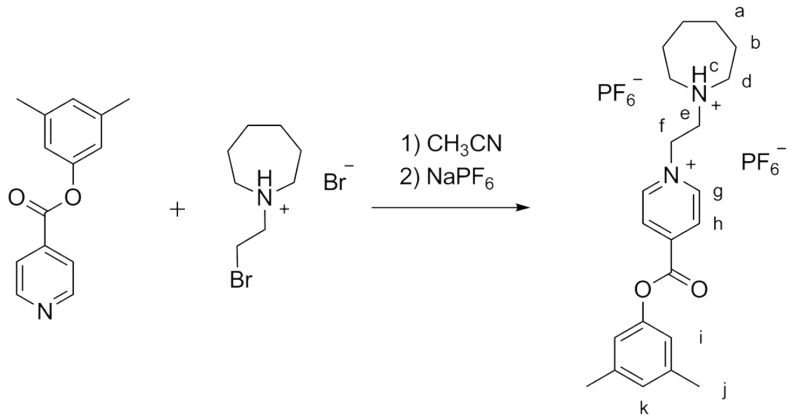

Scheme S2.9. Synthesis of the dumbbell [**1-Aze·H**][PF_6]$_2$.

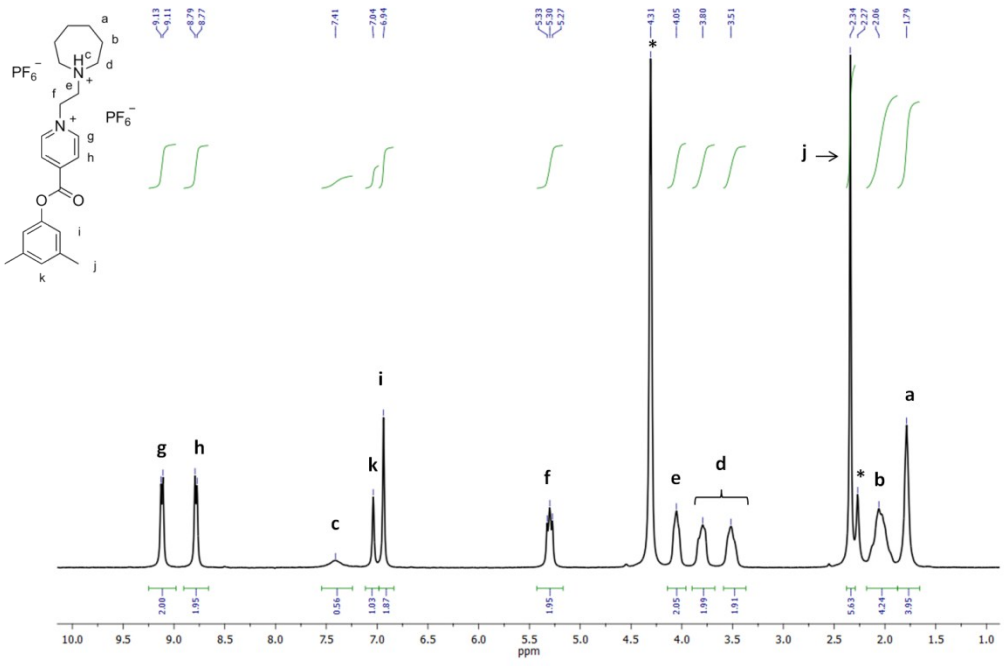

Figure S2.16. Assigned ^{1}H NMR spectrum of the dumbbell [**1-Aze·H**][PF_6]$_2$ (300MHz, CD_3NO_2, rt, * = residual solvents).

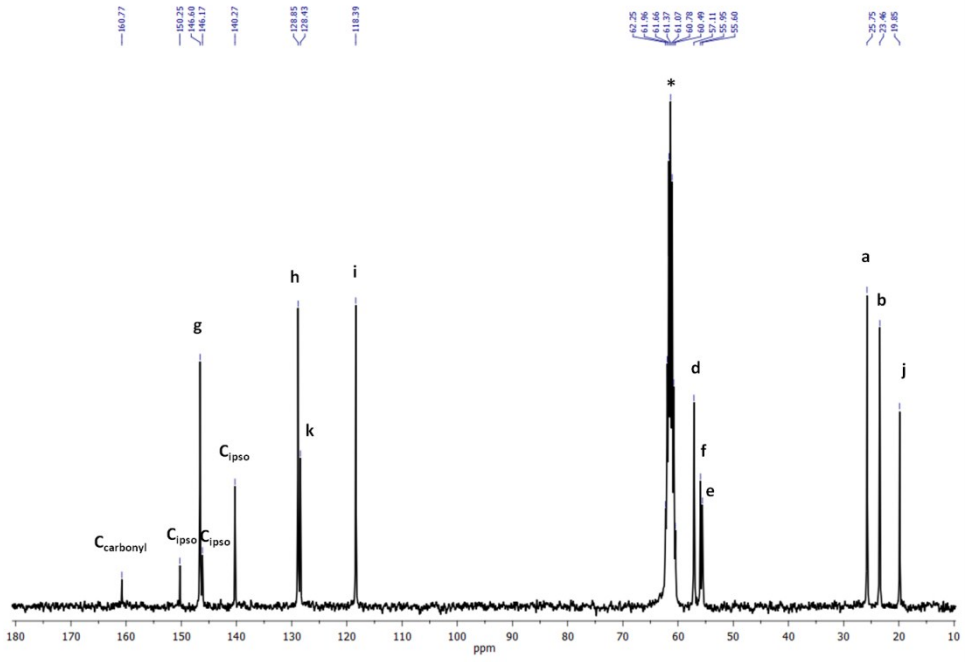

Figure S2.17. Assigned ^{13}C NMR spectrum of the dumbbell [**1-Aze·H**][PF_6]$_2$ (75MHz, CD_3NO_2, rt, * = residual solvent).

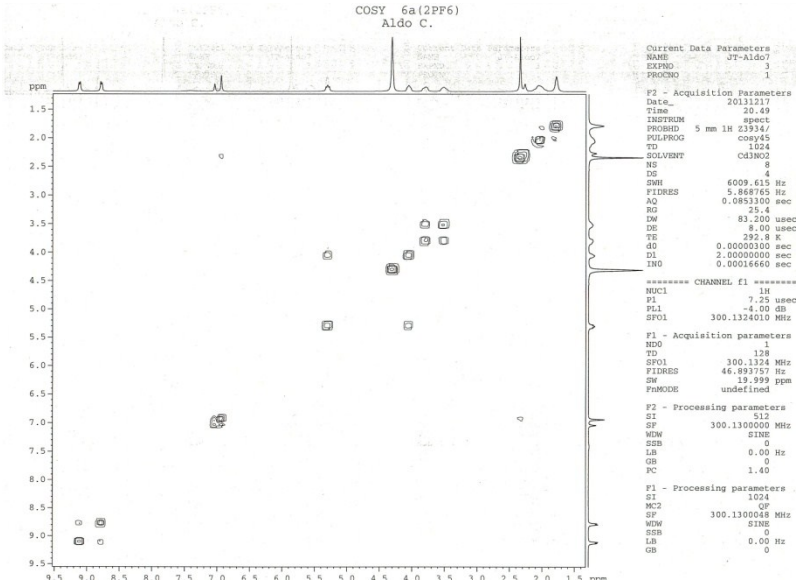

Figure S2.18. 2D NMR COSY of the dumbbell [**1-Aze·H**][PF_6]$_2$ (300MHz, CD_3NO_2, rt).

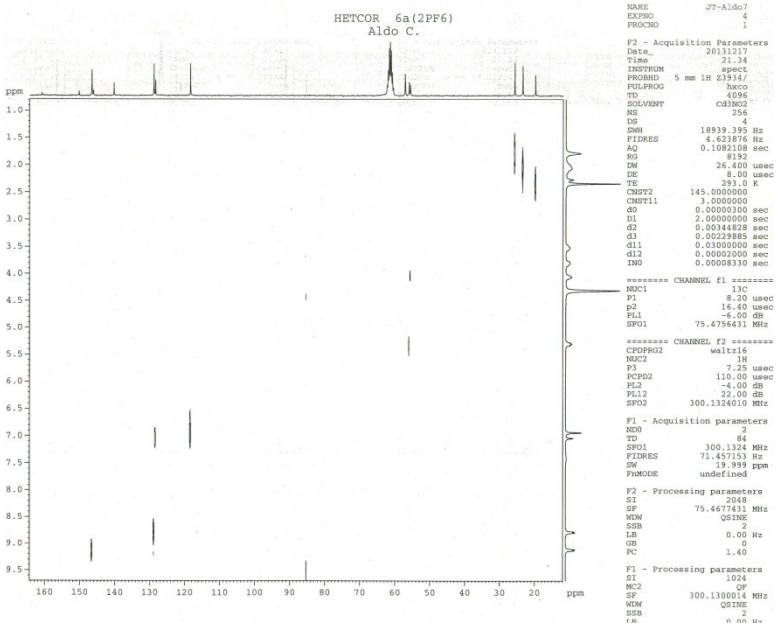

Figure S2.19. 2D NMR HETCOR of the dumbbell [**1-Aze·H**][PF_6]$_2$ (CD_3NO_2, rt).

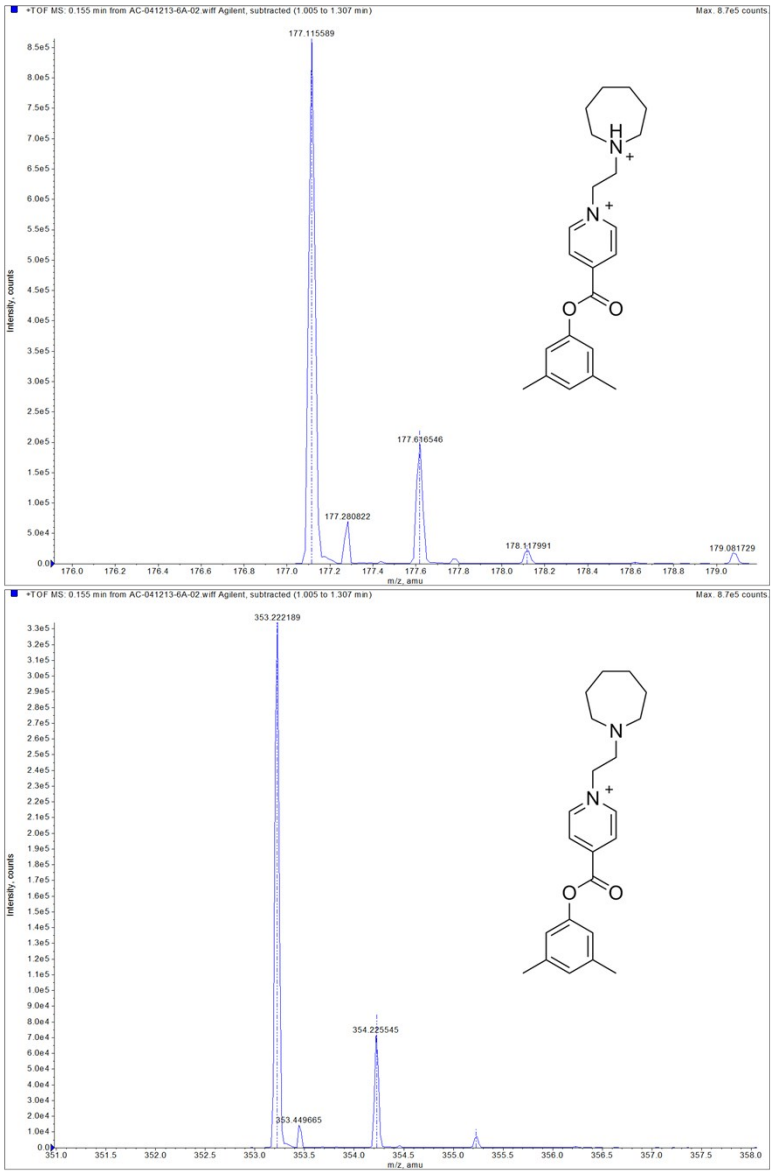

Figure S2.20. ESI-HRMS spectra of [**1-Aze·H**][PF_6]$_2$. Experimental molecular ion (continous line) and calculated isotopic profile (broken line).

Synthesis of [**1-Azo·H**][PF_6]$_2$. The 1-(2-bromoethyl)azocanium bromide was prepared from the corresponding amine by the same procedure described to obtain the 1-(2-bromoethyl)azepanium bromide, as depicted in Scheme S2.10 (0.82g, 52%).

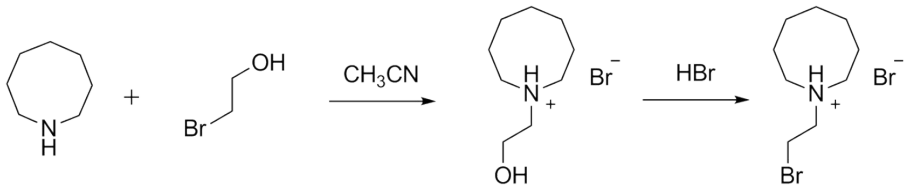

Scheme S2.10. Synthesis of 1-(2-bromoethyl)azocanium bromide.

Isonicotinate **INF** (0.58g, 2.55mmol), 1-(2-bromoethyl)azocanium bromide (0.40g, 1.33mmol) and CH_3CN (4mL) were refluxed for 1 day. The white solid was filtered and washed with $(CH_3)_2CO$ (0.34g, 49%). The bromide salt can be transformed into the hexafluorophosphate salt by ion exchange in the presence of 1 equivalent of HBr (0.34g, 80%). ^{1}H NMR (300 MHz, CD_3NO_2) δ_H 9.13 (2H, d, J = 6.3 Hz, H_h), 8.78 (2H, d, J = 6.2 Hz, H_i), 7.68 (1H, br.s, H_d), 7.04 (1H, s, H_l), 6.93 (2H, s, H_j), 5.30 (2H, t, J = 7.8 Hz, H_g), 4.04 (2H, t, J = 7.2 Hz, H_f), 3.76-3.55 (4H, br.m, H_e), 2.34 (6H, s, H_k), 2.12-2.00 (4H, br.m, H_c), 1.79 (6H, br.m, H_b and H_a). ^{13}C NMR (75 MHz, CD_3NO_2) δ_C 160.79 ($C_{carbonyl}$); 150.25 (C_{ipso}); 146.62 (C_h); 146.15 (C_{ipso}); 140.23 (C_{ipso}); 128.83 (C_i); 128.43 (C_l); 118.39 (C_j); 55.97 (C_g); 54.73 (C_f); 53.90 (C_e); 24.79 (C_b); 24.04 (C_a); 22.49 (C_c); 19.85 (C_k). ESI-HRMS: *m*/*z* found for [**1-Azo·H**]$^{2+}$ 184.122968, calculated 184.122640, error 1.777567ppm; *m*/*z* found for [**1-Azo**]$^{1+}$ 367.237650, calculated 367.238004, error -0.966555ppm.

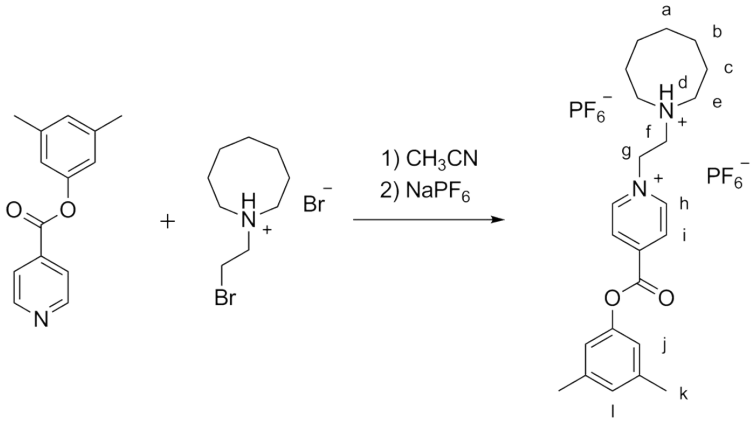

Scheme S2.11. Synthesis of the dumbbell [**1-Azo·H**][PF_6]$_2$.

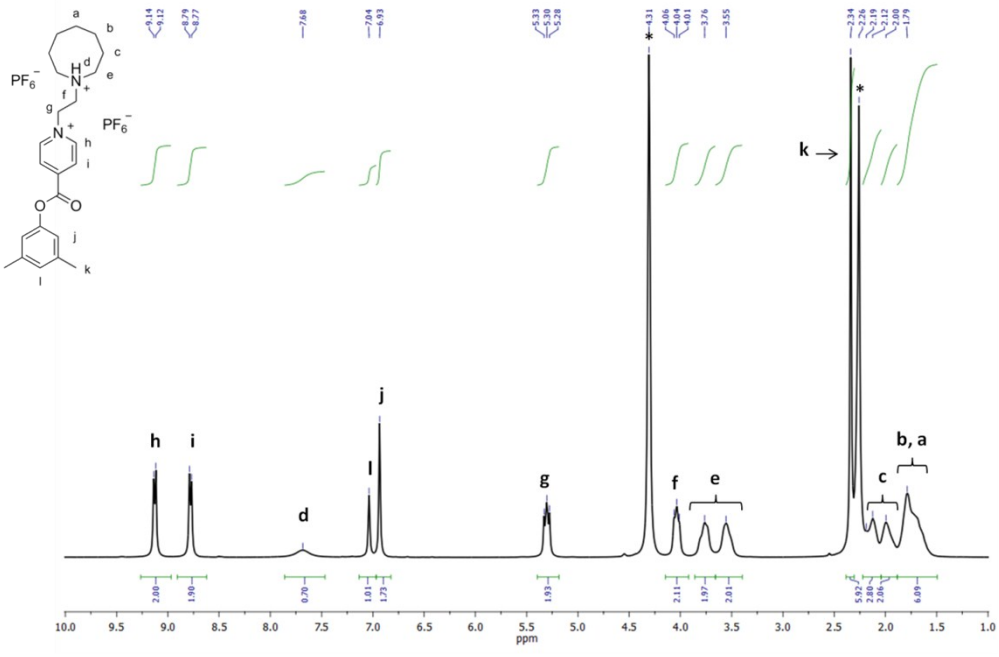

Figure S2.21. Assigned ^{1}H NMR spectrum of the dumbbell [**1-Azo·H**][PF_6]$_2$ (300MHz, CD_3NO_2, rt, * = residual solvents).

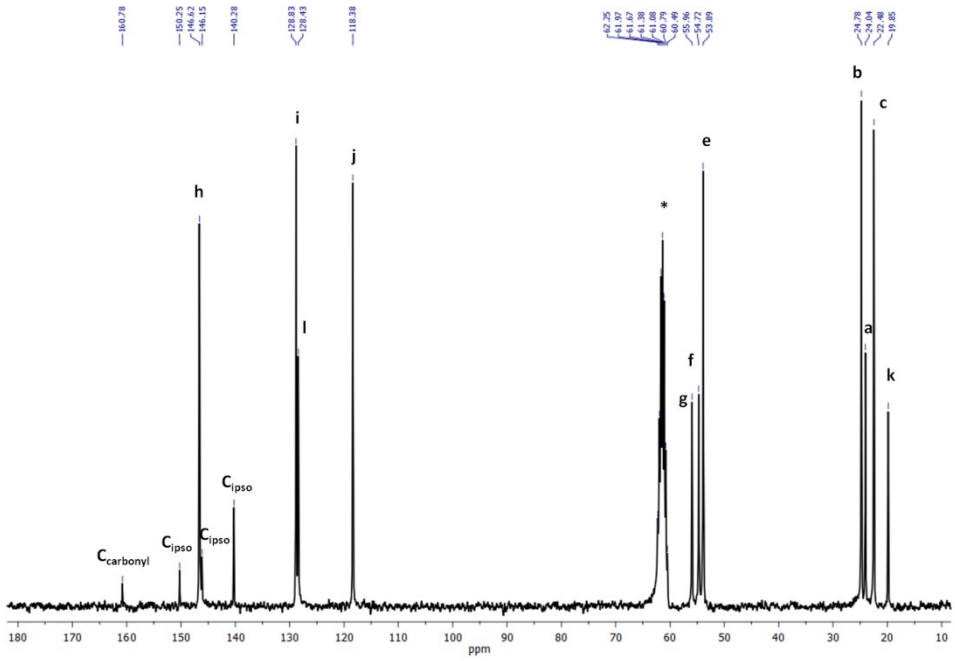

Figure S2.22. Assigned ^{13}C NMR spectrum of the dumbbell [**1-Azo·H**][PF_6]$_2$ (75MHz, CD_3NO_2, rt, * = residual solvent).

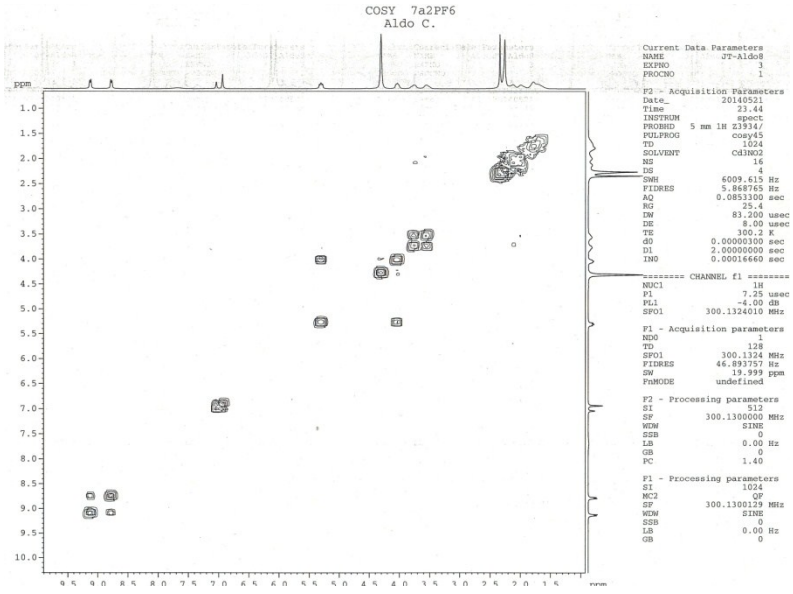

Figure S2.23. 2D NMR COSY of the dumbbell [**1-Azo·H**][PF_6]$_2$ (300MHz, CD_3NO_2, rt).

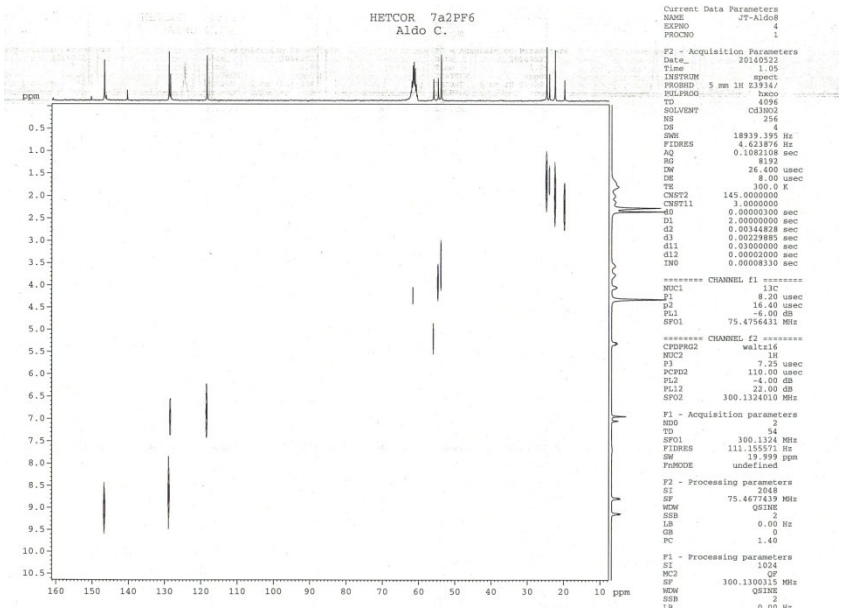

Figure S2.24. 2D NMR HETCOR of the dumbbell [**1-Azo·H**][PF_6]$_2$ (CD_3NO_2, rt).

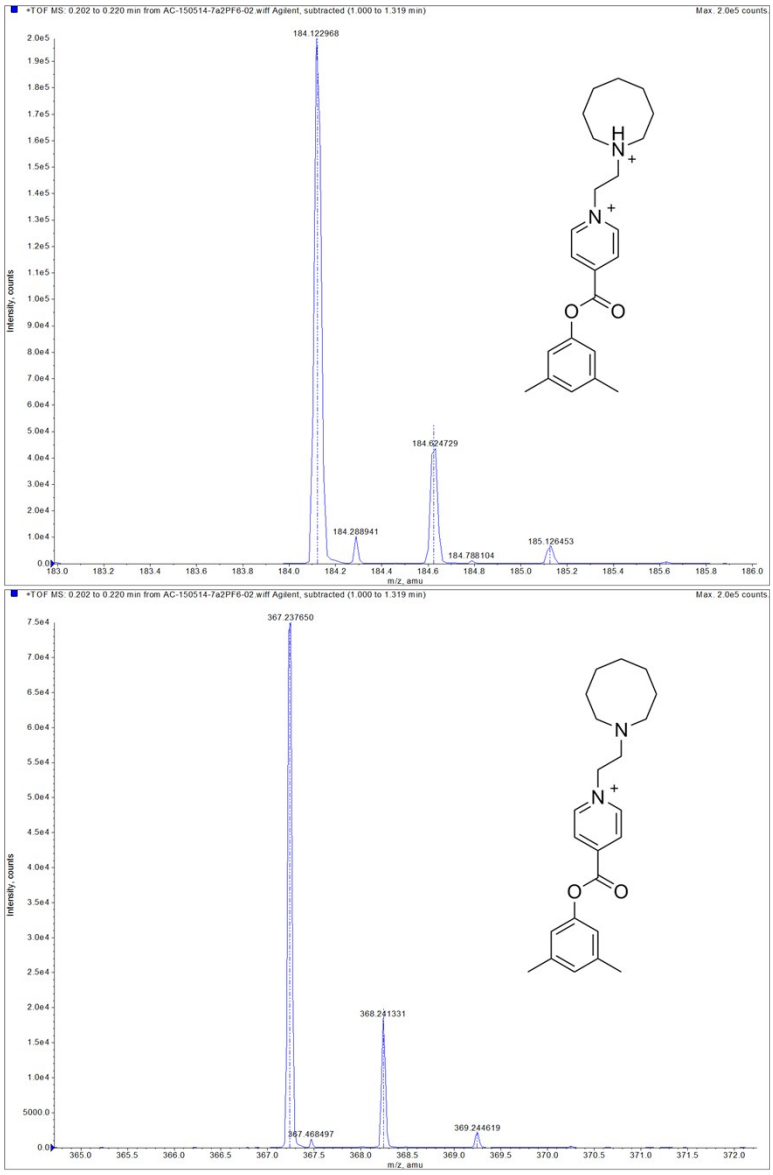

Figure S2.25. ESI-HRMS spectra of [**1-Azo·H**][PF_6]$_2$. Experimental molecular ion (continous line) and calculated isotopic profile (broken line).

Synthesis of [**2**][PF_6]. To a solution of piperidine (0.5mL, 5.04mmol) in CH_3CN (4mL) was added 1.4mL of (2-bromoethyl)benzene (10.05mmol). The mixture was refluxed for 3 days. The solid was filtered and washed repeatedly with cold CH_3CN (1.34g, 98%). The linear molecule, obtained as the bromide salt, could be transformed into the corresponding hexafluorophosphate salt by anion exchange (1.51g, 91%). ^{1}H NMR (500 MHz, CD_3NO_2) δ_H 7.37-7.23 (5H, m, H_g), 6.44 (1H, br.m, H_c), 3.75 (2H, br.d, H_e), 3.47-3.13 (4H, m, H_d), 3.10 (2H, br.m, H_f), 2.03-1.52 (4H, m, H_b and H_a). ^{13}C NMR (125 MHz, CD_3NO_2) δ_C 136.04 ($C_{g\ ipso}$); 129.00, 128.81, 127.39 (C_g); 58.42 (C_e); 54.24 (C_d); 29.93 (C_f); 23.01 (C_b); 21.18 (C_a). ESI-HRMS: *m*/*z* found for [**2**]$^{1+}$ 190.159023, calculated 190.159026, error -0.016975ppm.

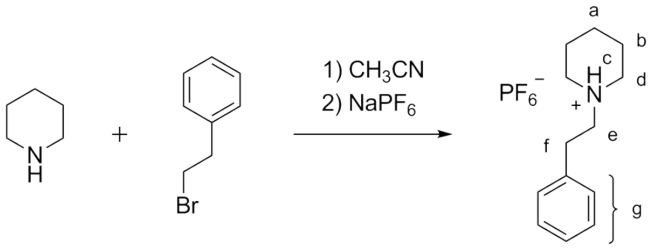

Scheme S2.12. Synthesis of the linear molecule [**2**][PF_6].

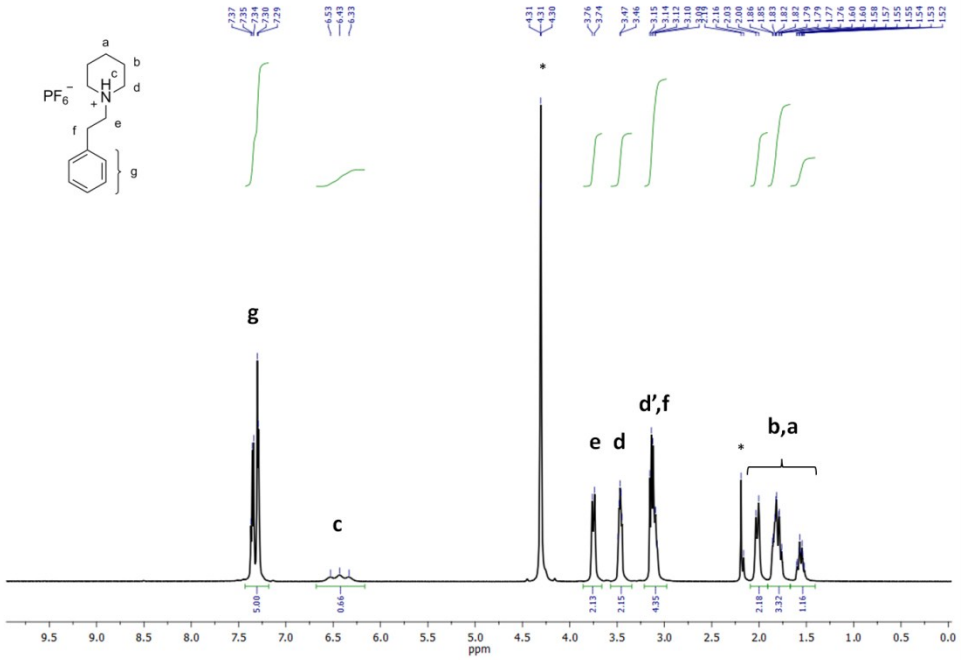

Figure S2.26. Assigned ^{1}H NMR spectrum of the dumbbell [**2**][PF_6] (500MHz, CD_3NO_2, rt, * = residual solvents).

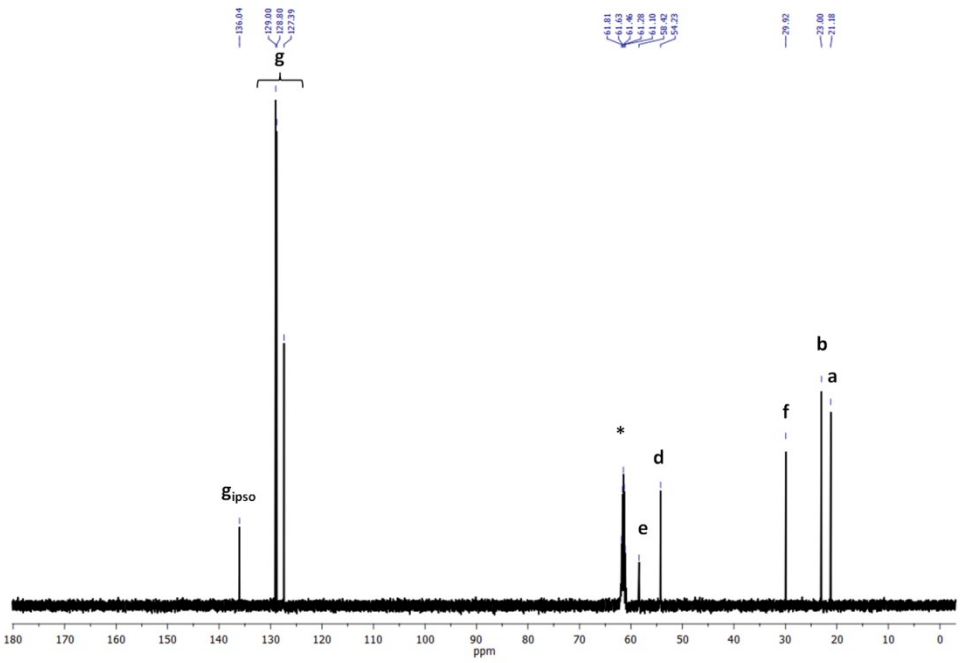

Figure S2.27. Assigned ^{13}C NMR spectrum of [**2**][PF_6] (125MHz, CD_3NO_2, rt, * = residual solvent).

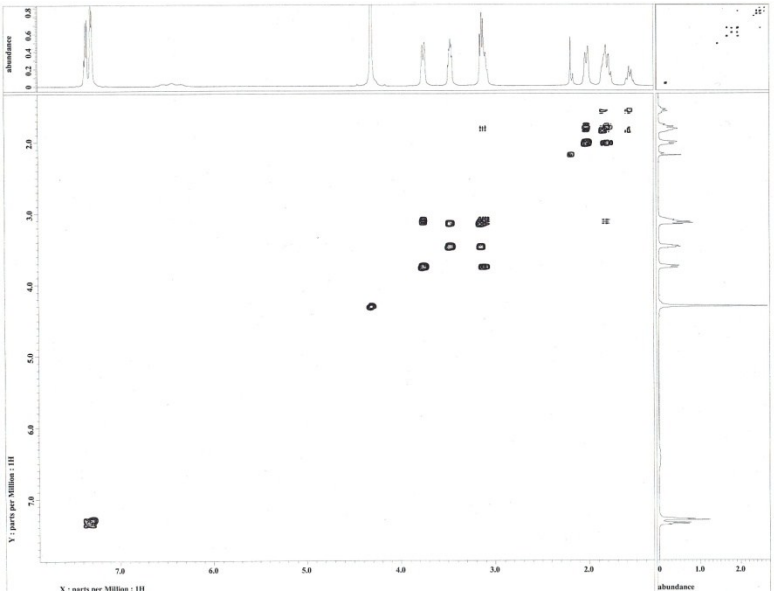

Figure S2.28. 2D NMR COSY of the linear molecule [**2**][PF_6] (500MHz, CD_3NO_2, rt).

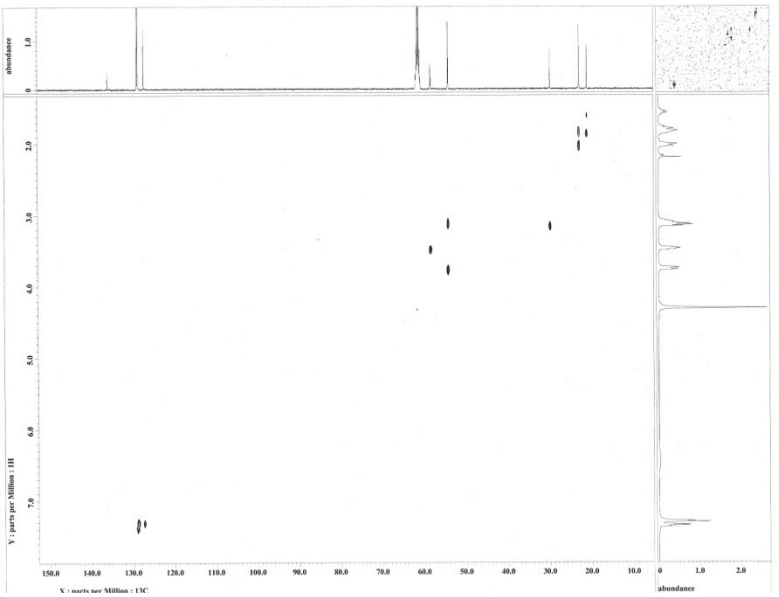

Figure S2.29. 2D NMR HETCOR of the linear molecule [**2**][PF_6] (CD_3NO_2, rt).

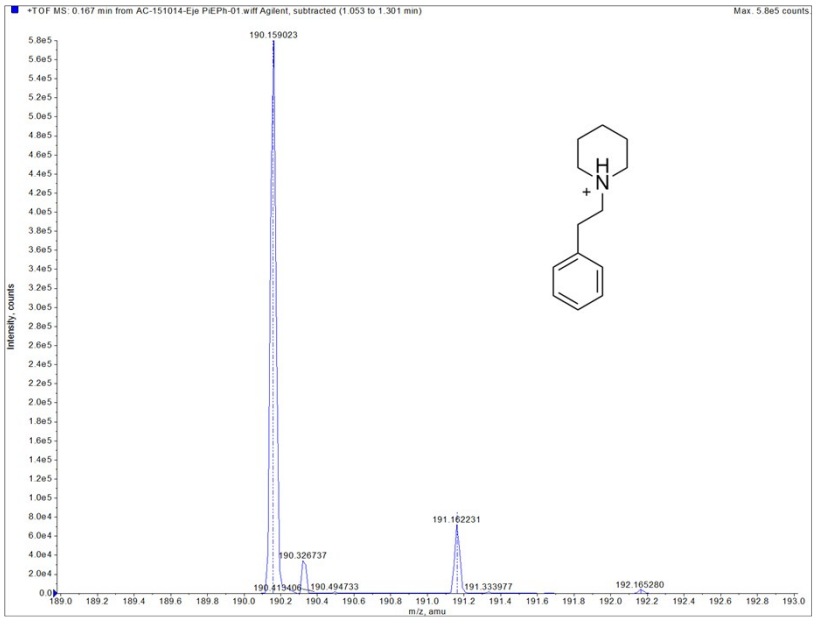

Figure S2.30. ESI-HRMS spectrum of [**2**][PF_6]. Experimental molecular ion (continous line) and calculated isotopic profile (broken line).

Synthesis of [**3**][PF_6]. To a solution of **INF** (0.51g, 2.24mmol) in CH_3CN (5mL) was added 1.56mL of (2-bromoethyl)benzene (11.22mmol). The mixture was refluxed for 5 days. The reaction mixture was allowed to reach the room temperature; the addition of an excess of diethyl ether promotes the formation of a yellow powder. The solid was filtered and washed repeatedly with hexane. The pale yellow solid was dried under vacuum (0.80g, 86%). This reaction yield the guest as the bromide salt, which can be easily transformed into the corresponding hexafluorophosphate salt by anion exchange (0.74, 80%). ^{1}H NMR (300 MHz, CD_3NO_2) δ_H 8.84 (2H, d, J = 6.4 Hz, H_d), 8.61 (2H, d, J = 6.0 Hz, H_e), 7.33-7.16 (5H, m, H_a), 7.03 (1H, s, H_h), 6.91 (2H, s, H_f), 5.05 (2H, t, J = 7.0 Hz, H_c),

3.44 (2H, t, J = 6.9 Hz, H_b), 2.33 (6H, s, H_g). ^{13}C NMR (75 MHz, CD_3NO_2) δ_C 161.01 ($C_{carbonyl}$); 150.28 (C_{ipso}); 145.61 (C_d); 144.98 ($H_{a\ ipso}$); 140.23 (C_{ipso}); 135.35 (C_{ipso}); 129.06, 128.83 (C_a); 128.36 (C_h); 127.97 (C_e); 127.59 (C_a); 118.46 (C_f); 63.94 (C_c); 36.87 (C_b); 19.87 (C_g). ESI-HRMS: m/z found for [**3**]$^{1+}$ 332.164543, calculated 332.164505, error 0.112630ppm.

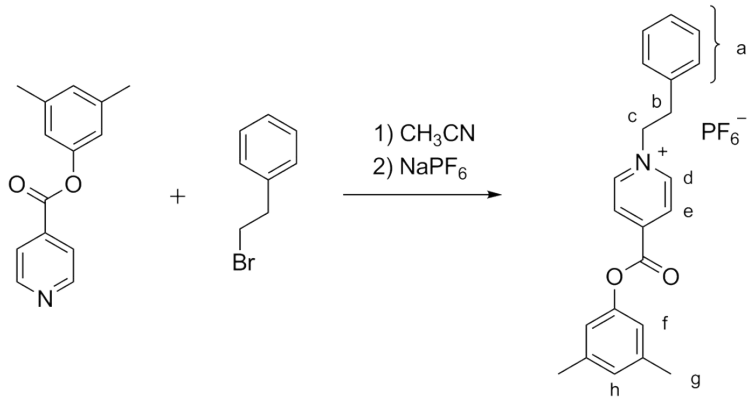

Scheme S2.13. Synthesis of the guest [**3**][PF_6].

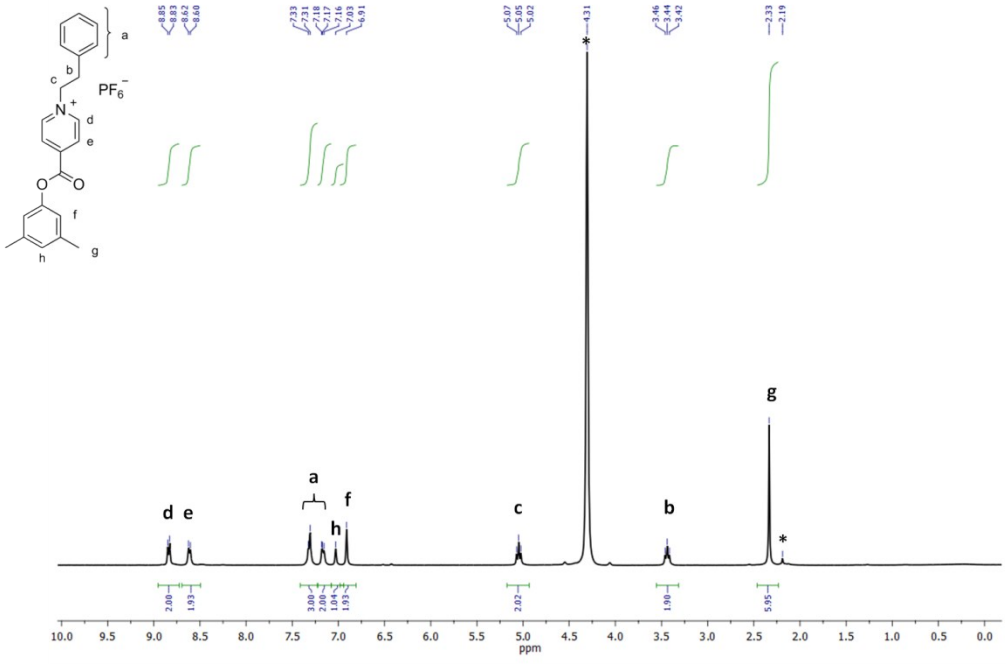

Figure S2.31. Assigned ^1H NMR spectrum of the guest [**3**][PF_6] (300MHz, CD_3NO_2, rt, * = residual solvents).

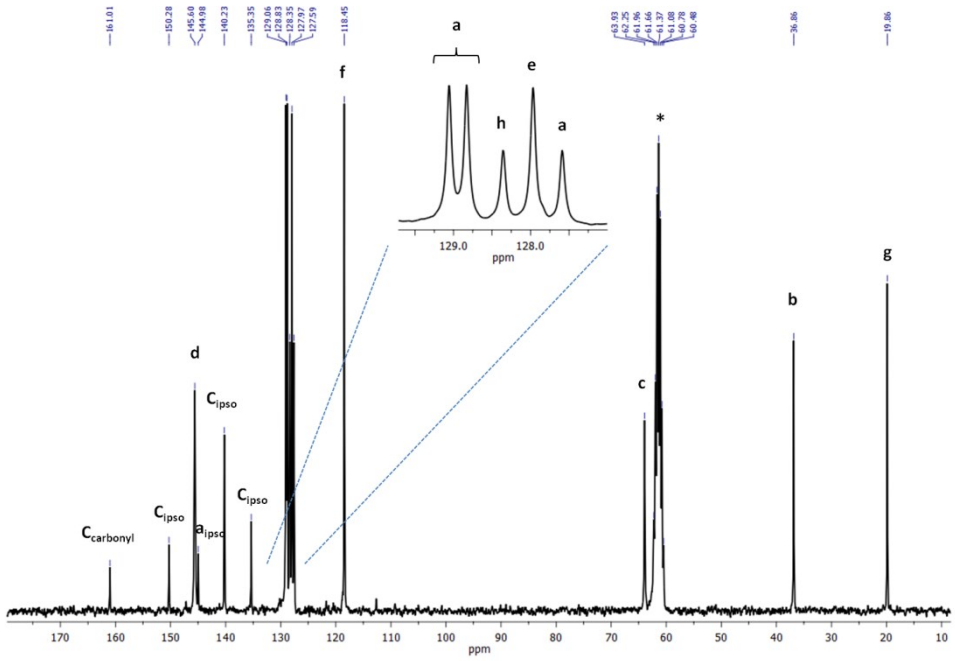

Figure S2.32. Assigned ^{13}C NMR spectrum of the guest [**3**][PF_6] (75MHz, CD_3NO_2, rt, * = residual solvent).

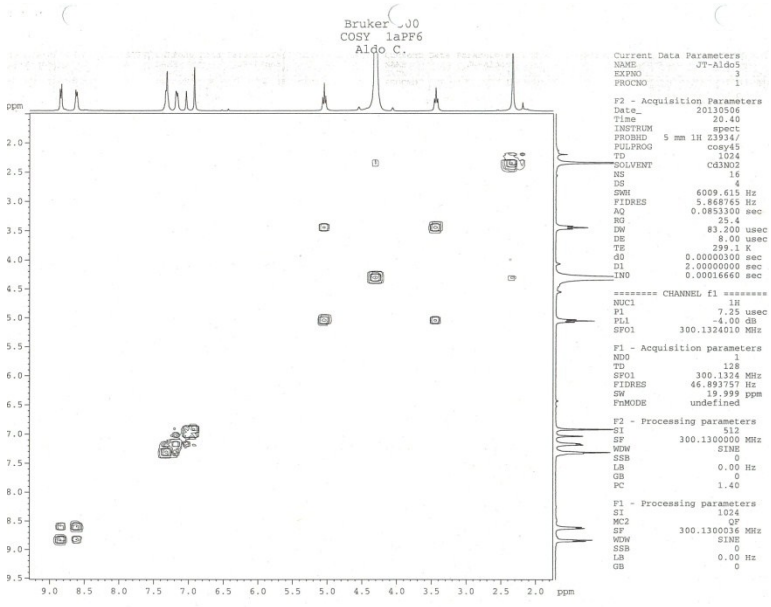

Figure S2.33. 2D NMR COSY of the guest [**3**][PF_6] (300MHz, CD_3NO_2, rt).

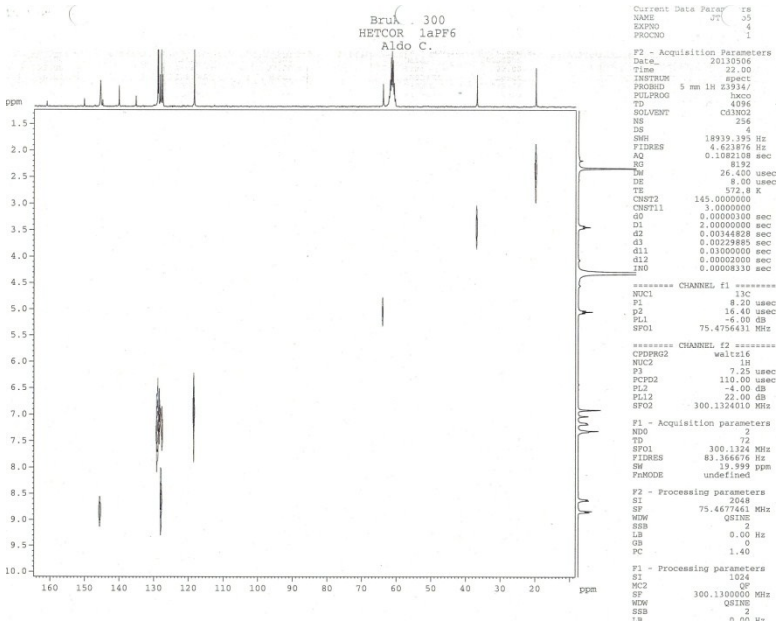

Figure S2.34. 2D NMR HETCOR of the guest [**3**][PF_6] (CD_3NO_2, rt).

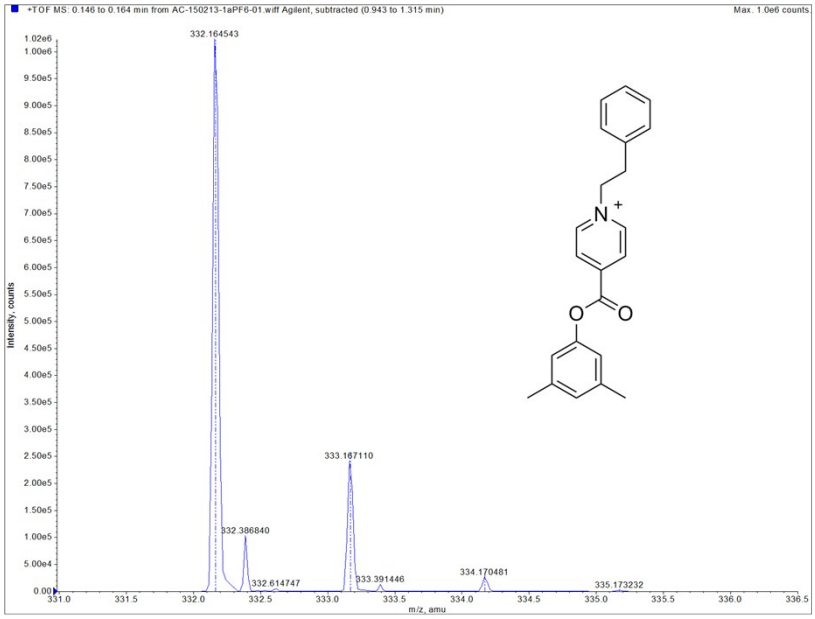

Figure S2.35. ESI-HRMS spectrum of [**3**][PF_6]. Experimental molecular ion (continous line) and calculated isotopic profile (broken line).

3. X-ray structure of $[1\text{-Pi}\cdot H]^{2+}$

Crystal data. $C_{21}H_{28}N_2O_2B_2F_8$, M = 514.07, triclinic, a = 6.8103(2), b= 12.0335(4), c = 15.7289(5) Å, U = 1191.39(7) Å^3, T = 173(2) K, space group P-1 (no.2), Z = 2, 5394 reflections measured, 4096 unique (R^{int} = 0.0567), which were used in all calculations. The final w$R(F^2)$ was 0.1678 (all data).

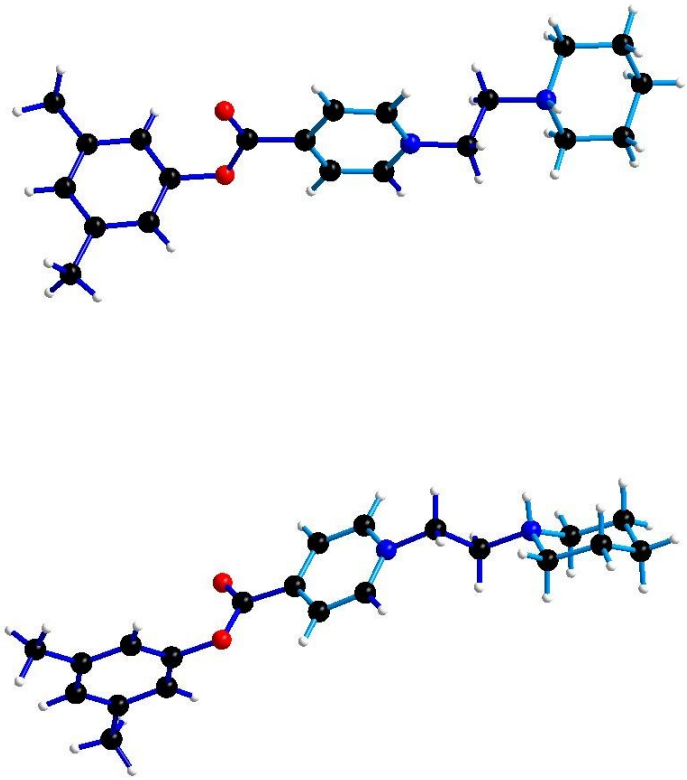

Fig. S3.1. X-Ray crystal structure. Ball-and-stick representations for the dumbbell $[\mathbf{1\text{-Pi}\cdot H}]^{2+}$. Anions are omitted. Carbon = black, oxygen = red, nitrogen = blue, hydrogen = white.

4. Cycles dimensions

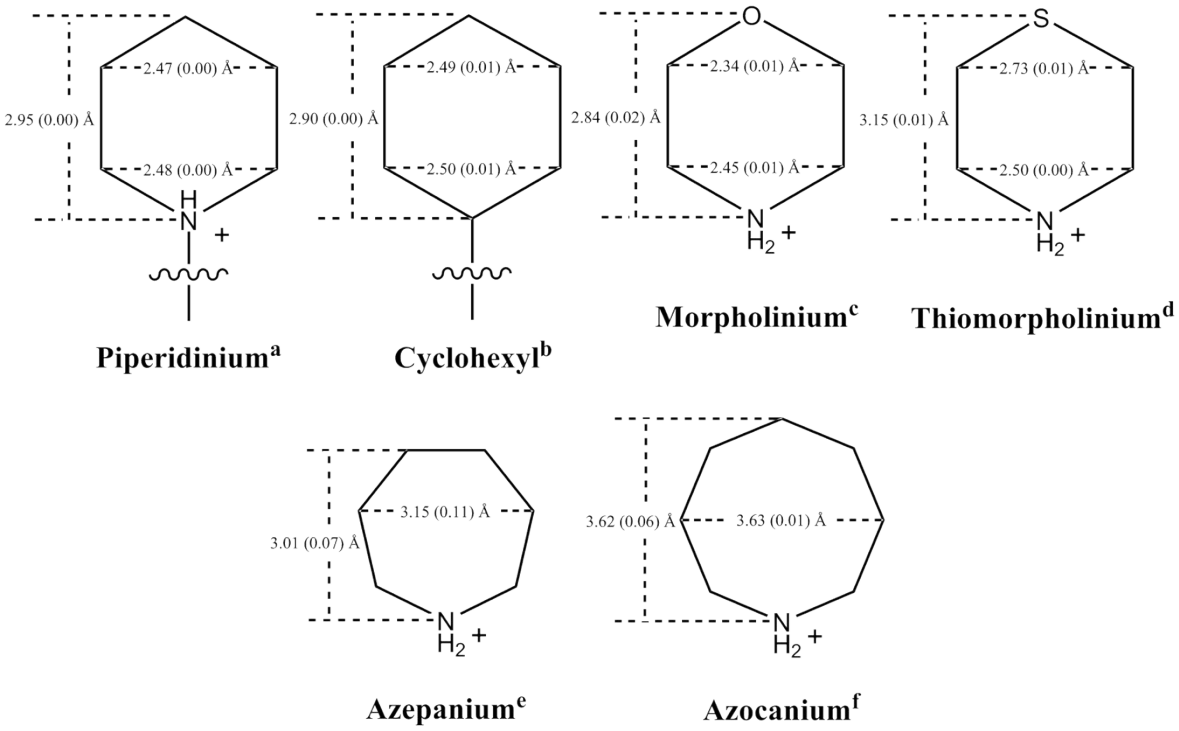

Piperidinium[a] **Cyclohexyl**[b] **Morpholinium**[c] **Thiomorpholinium**[d]

Azepanium[e] **Azocanium**[f]

[a] Values (std. dev.) from [**1-Pi·H**]$^{2+}$ X-ray structure.

[b] Average values (std. dev.) from CCDC X-ray structures: CORYAD, SERWIV.

[c] Average values (std. dev.) from CCDC X-ray structures: BIYDUK, BIYGAT, JILWUW.

[d] Average values (std. dev.) from CCDC X-ray structures: AZOVOB, KOFBUE, KOFCAL.

[e] Average values (std. dev.) from CCDC X-ray structures: HEXAMC, VANRAD, XIMBZA, XIMBZB.

[f] Average values (std. dev.) from CCDC X-ray structures: HEPAMC, XOJZUT.

5. NMR solution behaviour and HR-MS

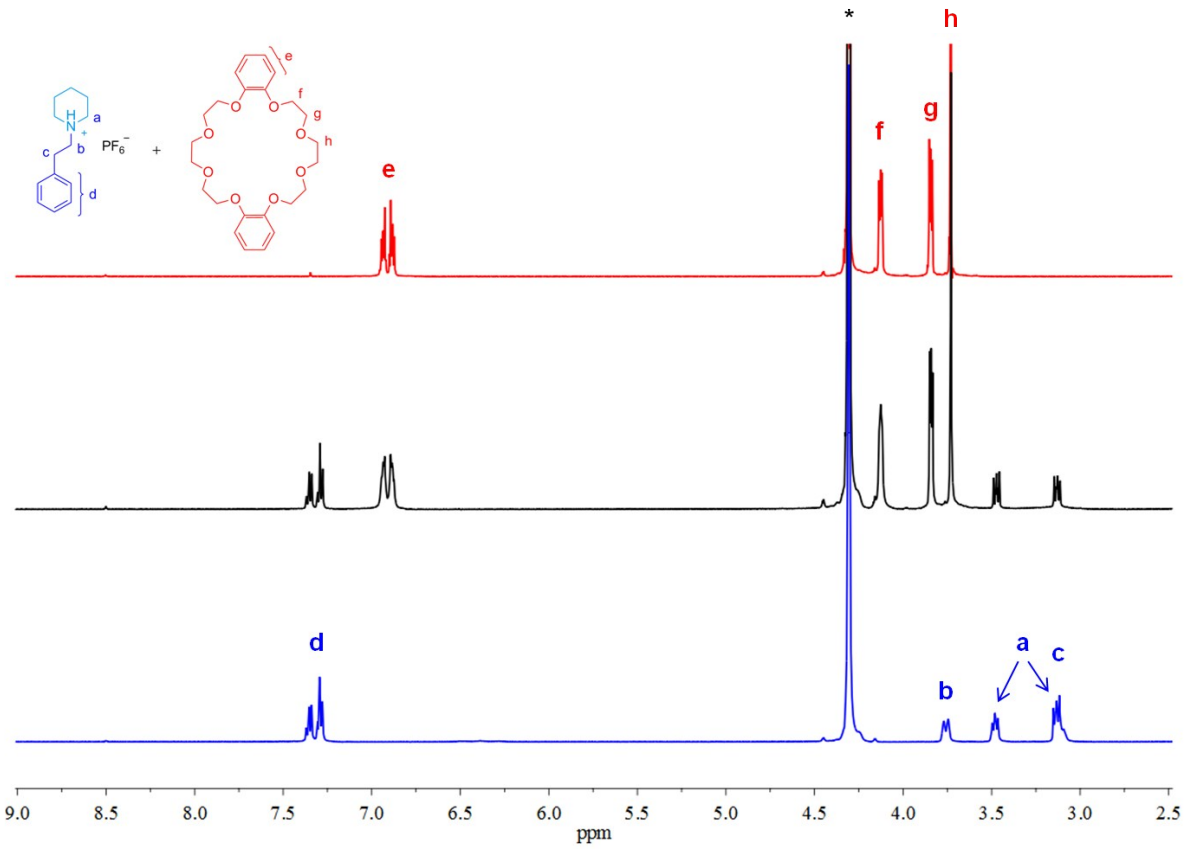

Fig. S5.1. Partial ^{1}H NMR spectra (500 MHz, CD_3NO_2, 20 °C, [guest] = [host] = 10^{-2} M). There was no evidence of the formation of an interpenetrated complex from the individual components [**2**][PF_6] and **DB24C8** (K_a ~ 0 M^{-1}). From bottom to top: free guest, mixture, and free host (* = residual solvent).

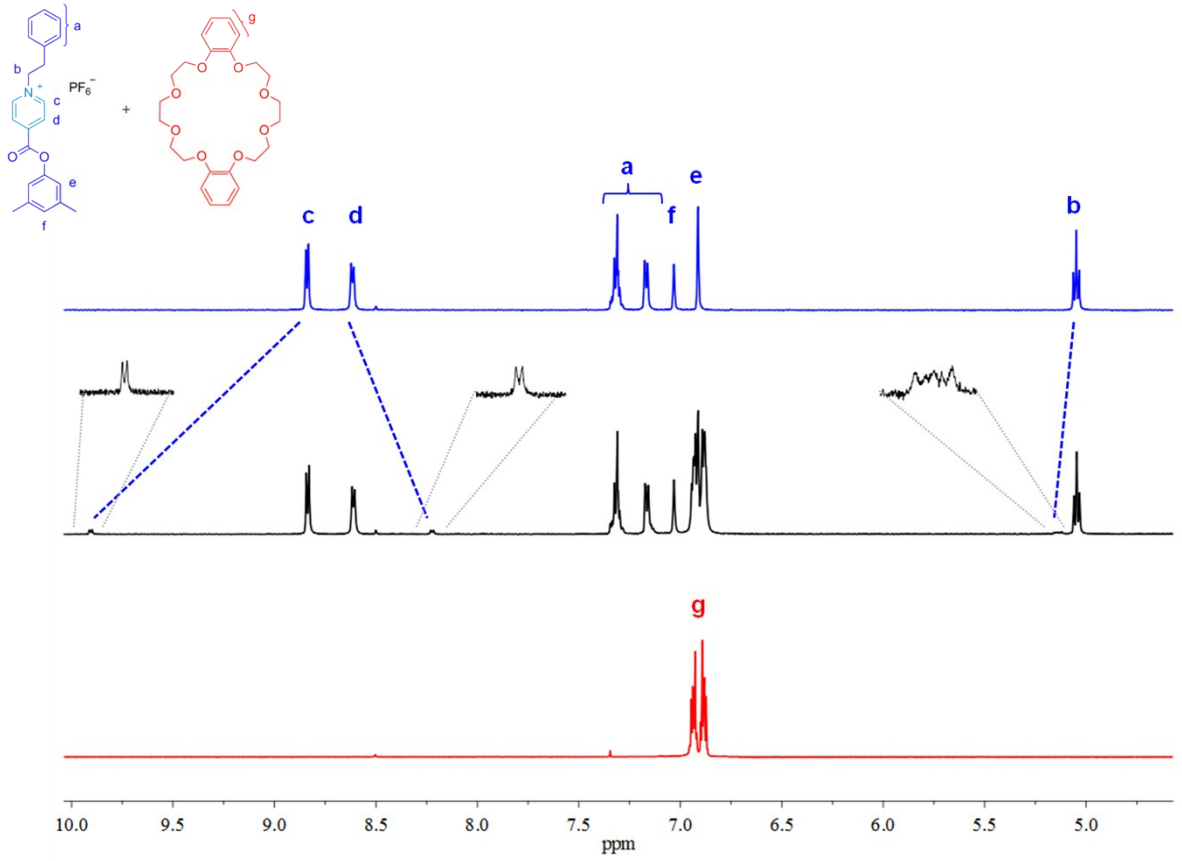

Fig. S5.2. Partial ^{1}H NMR spectra (500MHz, CD_3NO_2, 20° C, [guest] = [host] = 10^{-2} M) showing the formation of the complex [**3**⊂DB24C8][PF_6] from [**3**][PF_6] and **DB24C8**. The equilibrium was reached immediately. From bottom to top: free host, mixture, and free guest. Blue lines relate the resonances for complex with those from free components.

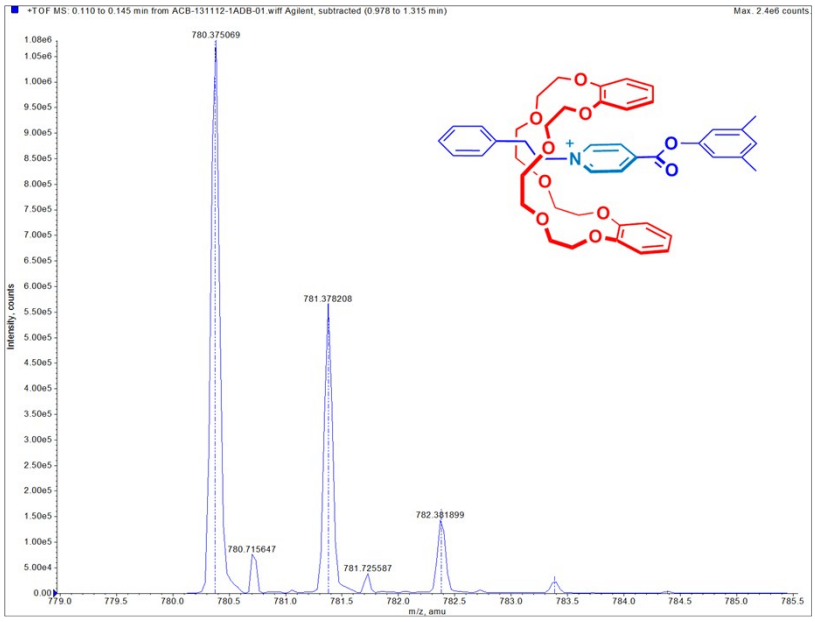

Figure S5.3. ESI-HRMS spectrum of [**3**⊂DB24C8][PF_6]. *m/z* found for [**3**⊂DB24C8]$^{1+}$ 780.375069, calculated 780.374223, error 1.082827ppm. Experimental molecular ion (continous line) and calculated isotopic profile (broken line).

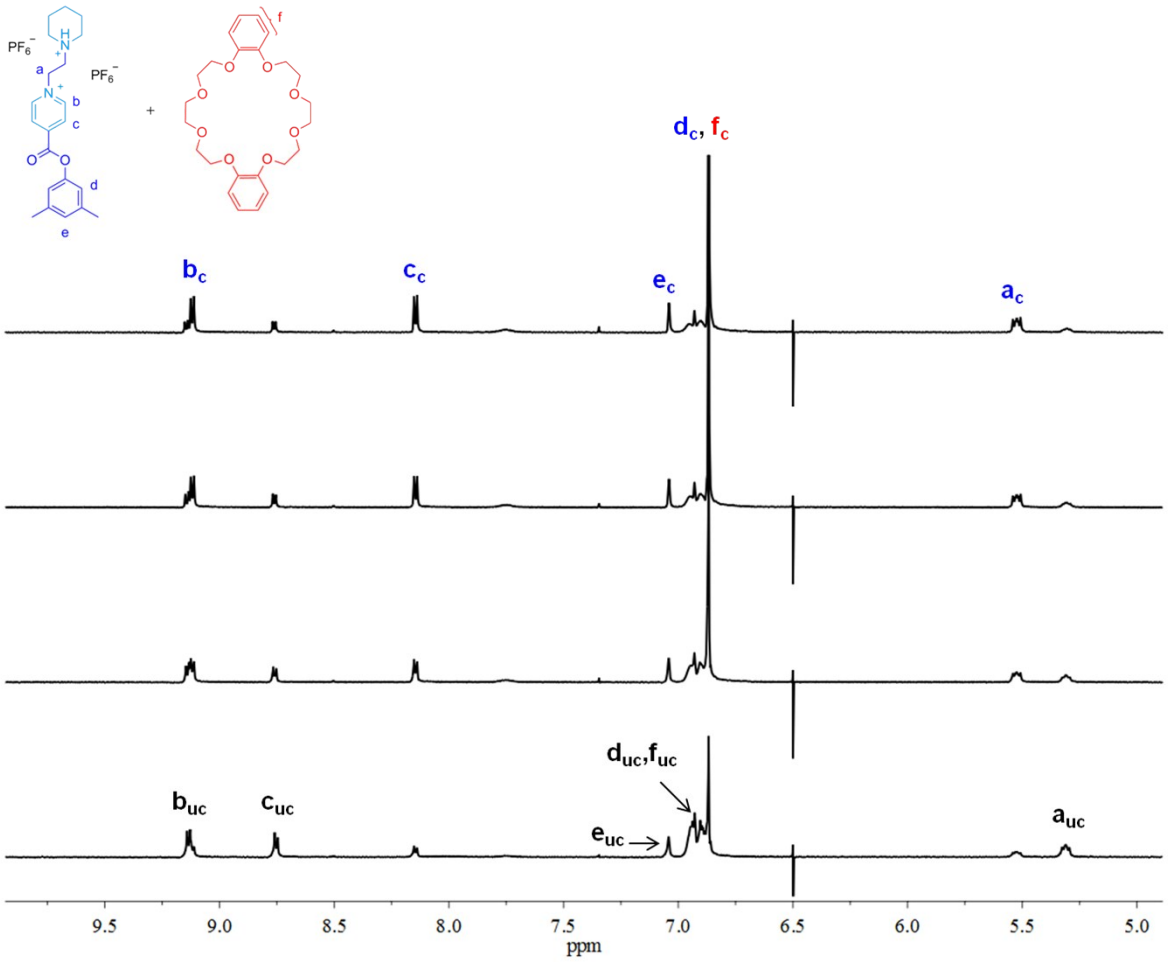

Fig. S5.4. Partial ^{1}H NMR spectra (500 MHz, CD_3NO_2, 20 °C, [guest] = [host] = 10^{-2} M) showing the formation of the complex [**1-Pi·H**⊂DB24C8][PF_6]$_2$ from [**1-Pi·H**][PF_6]$_2$ and **DB24C8** by slippage. From bottom to top, approximate time = 3, 8, 14, 21 minutes (uc = uncomplexed; c = complexed).

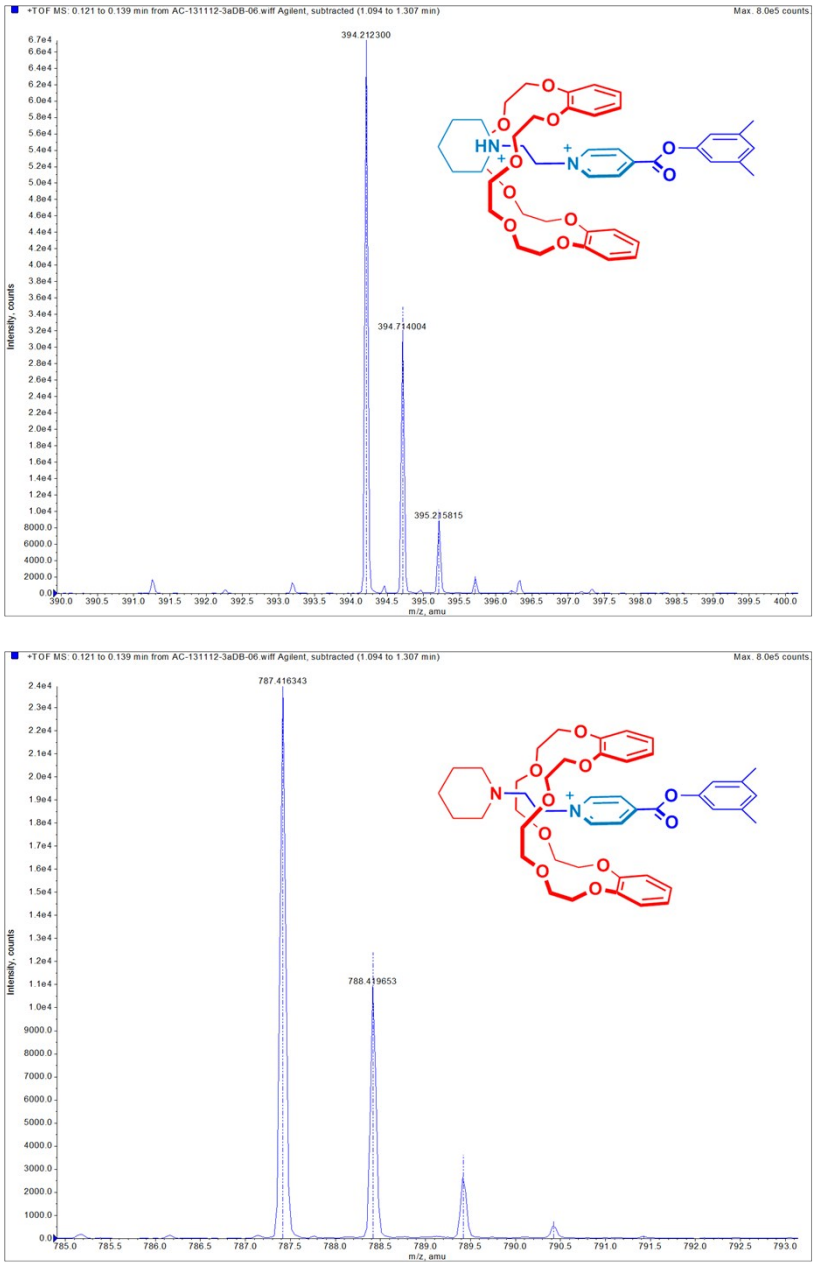

Figure S5.5. ESI-HRMS spectra of [**1-Pi·H**⊂DB24C8][PF_6]$_2$. *m/z* found for [**1-Pi·H**⊂DB24C8]$^{2+}$ 394.212300, calculated 394.211849, error 1.141951ppm; *m/z* found for [**1-Pi**⊂DB24C8]$^{1+}$ 787.416343, calculated 787.416423, error -0.101846ppm. Experimental molecular ion (continous line) and calculated isotopic profile (broken line).

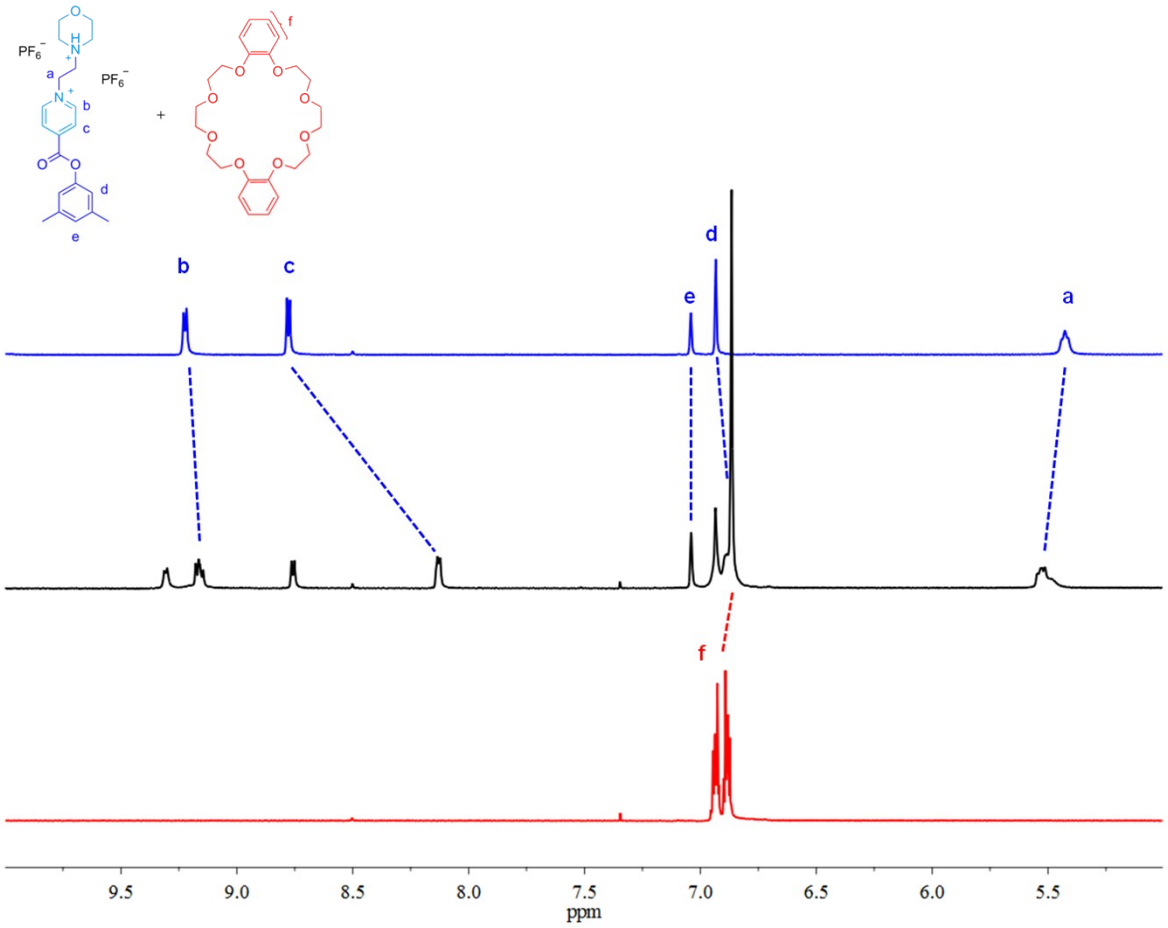

Fig. S5.6. Partial ^{1}H NMR spectra (500MHz, CD_3NO_2, 20° C, [guest] = [host] = 10^{-2} M) showing the formation of the complex [**1-Mp·H**⊂DB24C8][PF_6]$_2$ from [**1-Mp·H**][PF_6]$_2$ and **DB24C8**. The equilibrium was reached immediately. From bottom to top: free host, mixture, and free dumbbell. Lines relate the resonances for complex with those from free components.

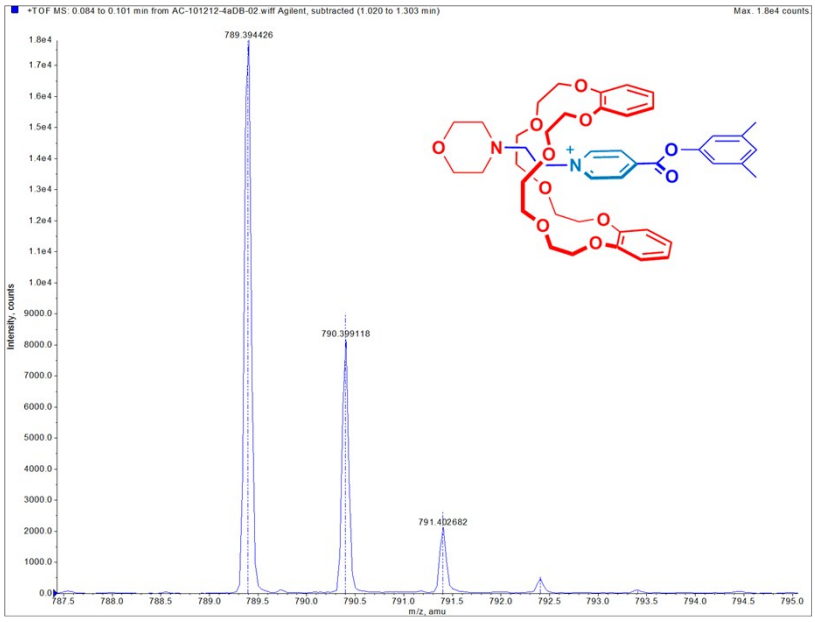

Figure S5.7. ESI-HRMS spectrum of [**1-Mp·H**⊂DB24C8][PF_6]. *m/z* found for [**1-Mp**⊂DB24C8]$^{1+}$ 789.394426, calculated 789.395687, error -1.598383ppm. Experimental molecular ion (continous line) and calculated isotopic profile (broken line).

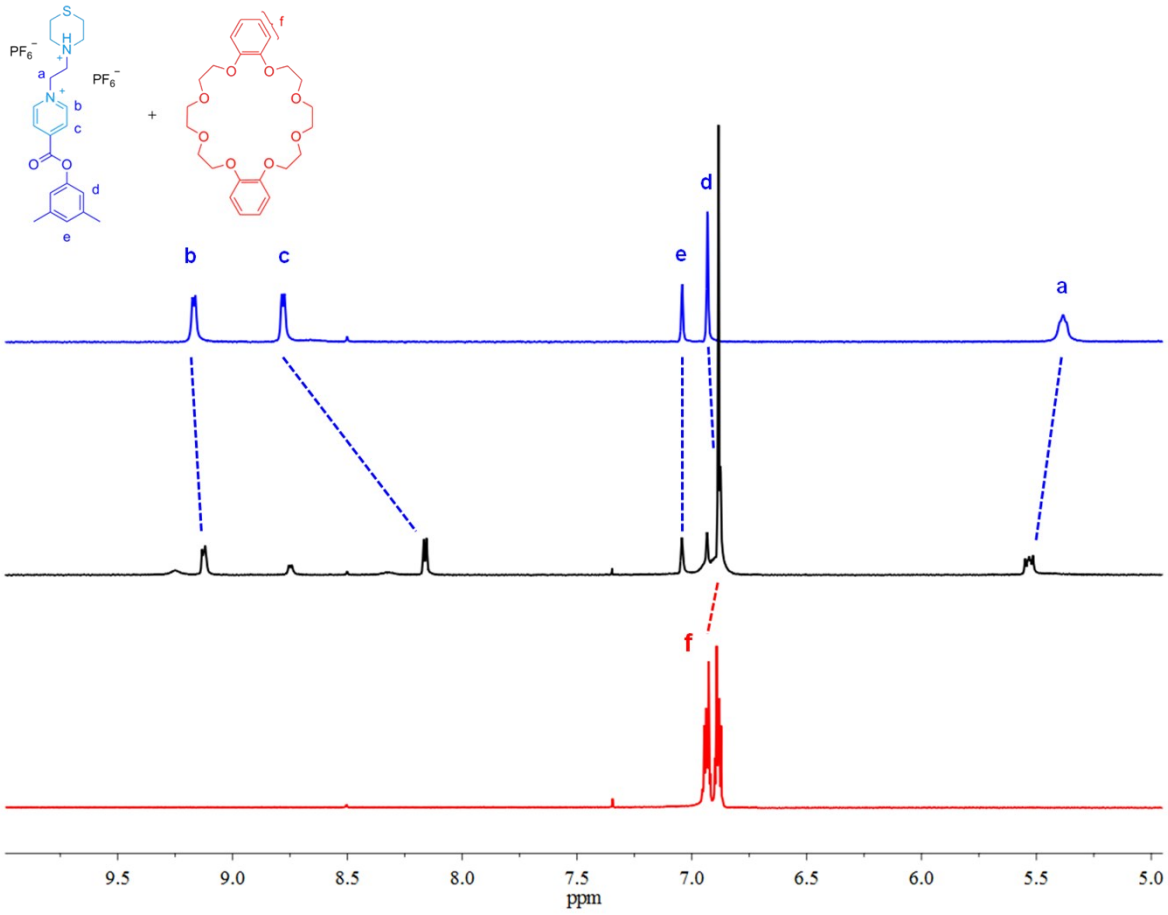

Fig. S5.8. Partial ^{1}H NMR spectra (500MHz, CD_3NO_2, 20° C, [guest] = [host] = 10^{-2} M) showing the formation of the complex [**1-Tm·H**⊂DB24C8][PF_6]$_2$ from [**1-Tm·H**][PF_6]$_2$ and **DB24C8**. The equilibrium was reached approximately 25 minutes after mixing. From bottom to top: free macrocycle, mixture, and free dumbbell. Lines relate the resonances for complex with those from free components.

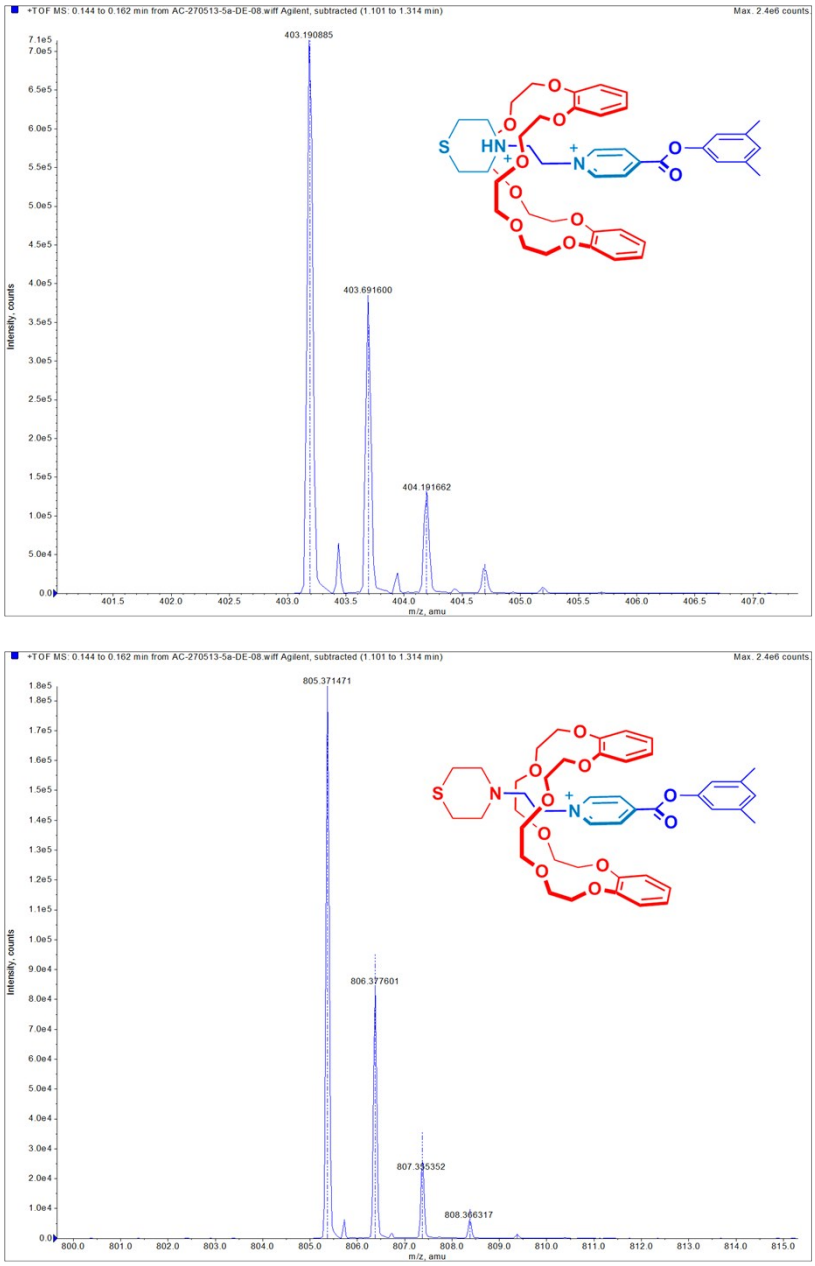

Figure S5.9. ESI-HRMS spectra of [**1-Tm·H**⊂DB24C8][PF_6]$_2$. *m/z* found for [**1-Tm·H**⊂DB24C8]$^{2+}$ 403.190885, calculated 403.190060, error 2.044468; *m/z* found for [**1-Tm**⊂DB24C8]$^{1+}$ 805.371471, calculated 805.372844, error -1.705939ppm. Experimental molecular ion (continous line) and calculated isotopic profile (broken line).

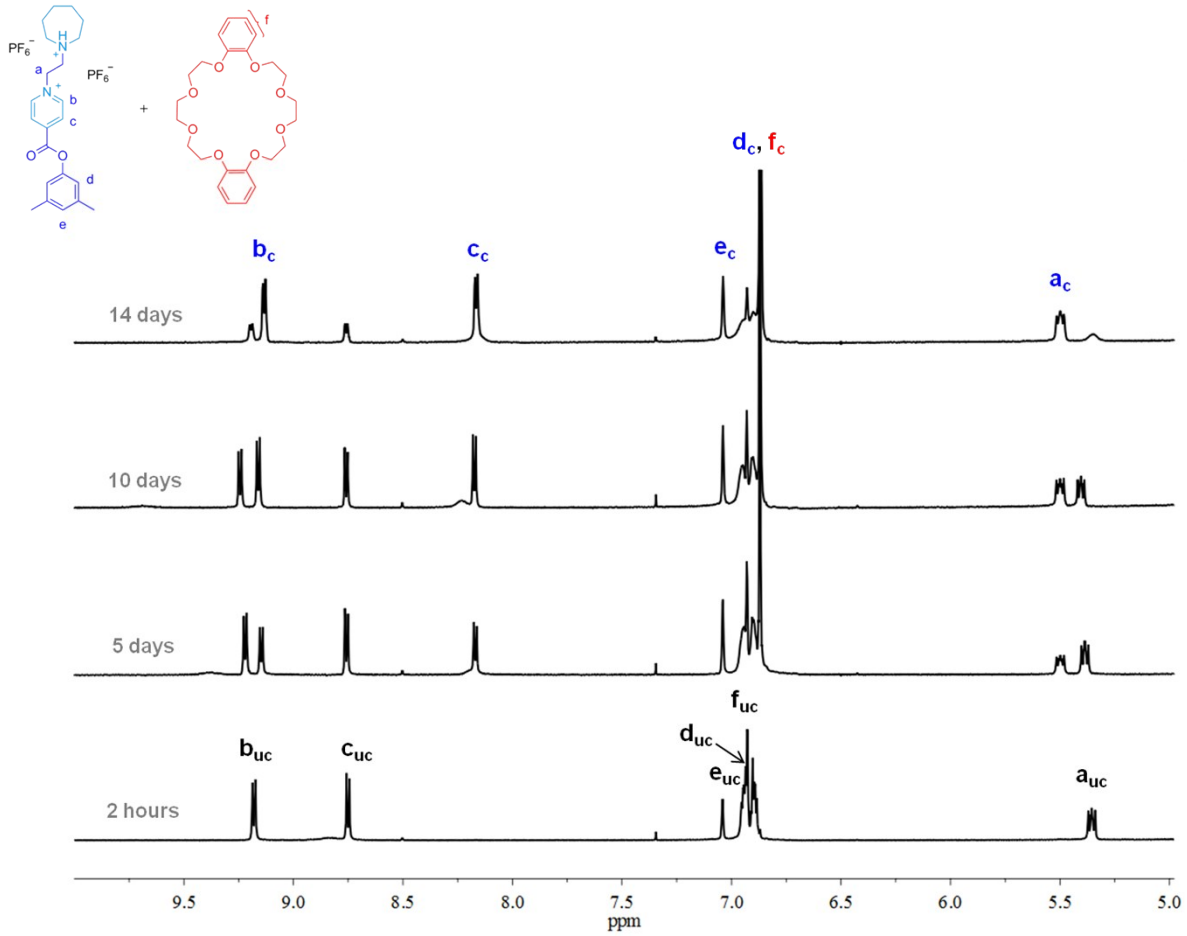

Fig. S5.10. Partial ^{1}H NMR spectra (500 MHz, CD_3NO_2, 20 °C, [guest] = [host] = 10^{-2} M) showing the formation of the complex [**1-Aze·H**⊂DB24C8][PF_6]$_2$ from [**1-Aze·H**][PF_6]$_2$ and **DB24C8** by slippage. The equilibrium was attained approximately 14 days after mixing (uc = uncomplexed; c = complexed).

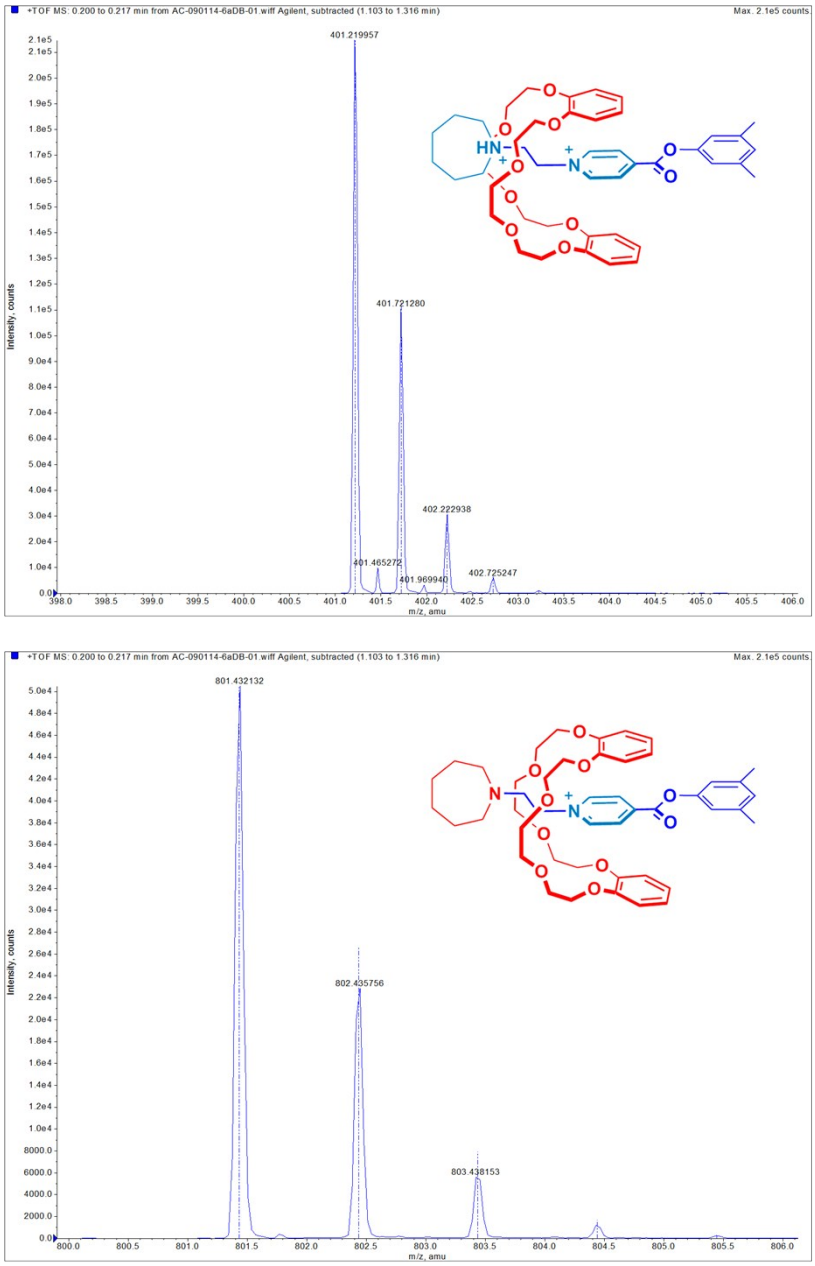

Figure S5.11. ESI-HRMS spectra of [**1-Aze·H**⊂DB24C8][PF_6]$_2$. *m/z* found for [**1-Aze·H**⊂DB24C8]$^{2+}$ 401.219957, calculated 401.219674, error 0.703184; *m/z* found for [**1-Aze**⊂DB24C8]$^{1+}$ 801.432132, calculated 801.432073, error 0.073273ppm. Experimental molecular ion (continous line) and calculated isotopic profile (broken line).

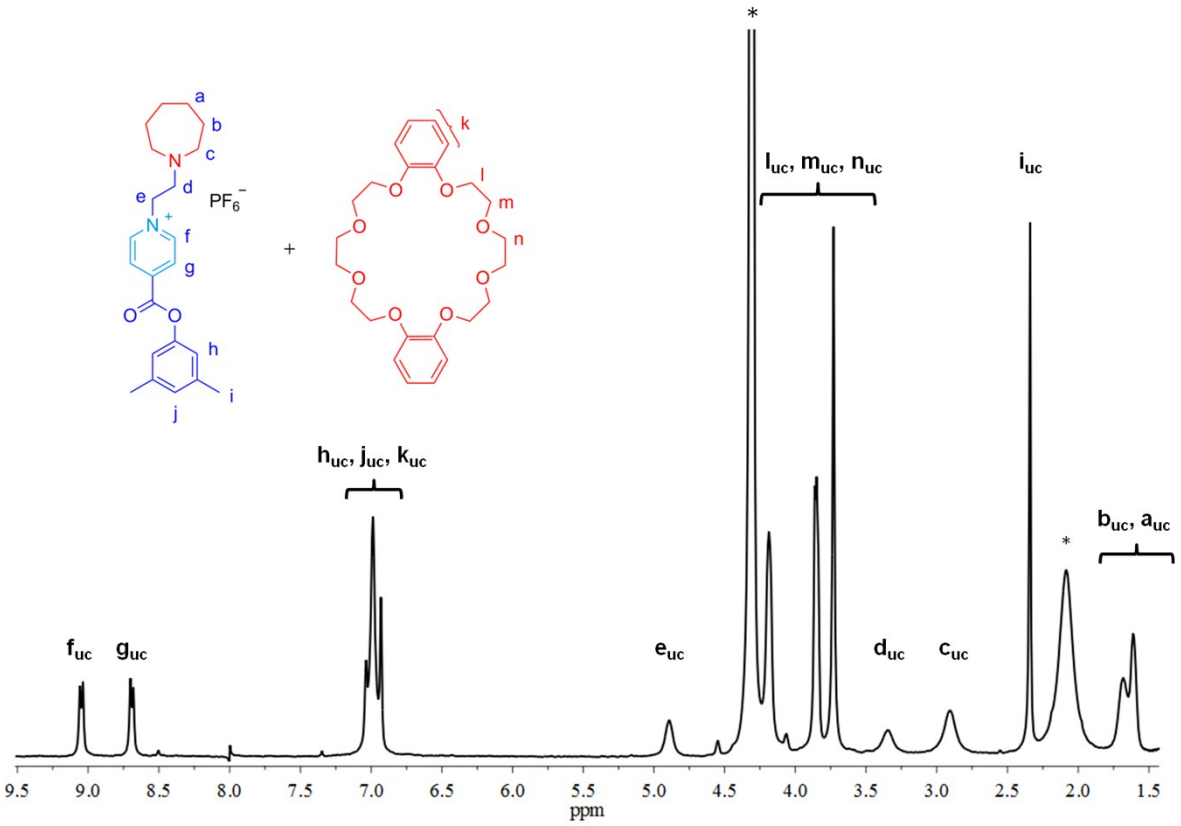

Fig. S5.12. ^{1}H NMR spectrum of an equimolar solution of [**1-Aze**][PF_6] and **DB24C8** (300 MHz, CD_3NO_2, 20 °C, 10^{-2} M). There was no evidence of association from the individual components after twenty two days (uc = uncomplexed; * = residual solvent).

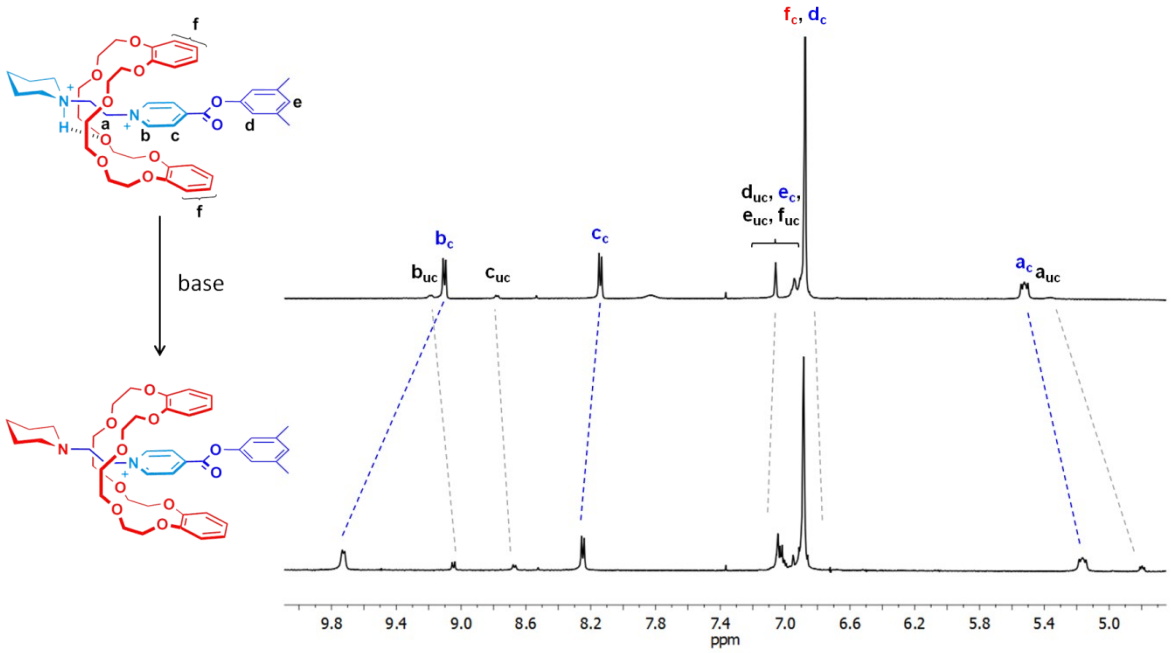

Fig. S5.13. Partial ^{1}H NMR spectra (400 MHz, CD_3NO_2, 20 °C, 10^{-2} M) of an equimolar solution of [**1-Pi·H**][PF_6]$_2$ and **DB24C8**: (top) when the equilibrium had been reached, (bottom) the same NMR sample after the addition of one equivalent of base; showing a different geometry for the deprotonated complex [**1-Pi**⊂DB24C8][PF_6]. Lines highlight the changes on the resonances upon base addition (uc = uncomplexed; c = complexed).

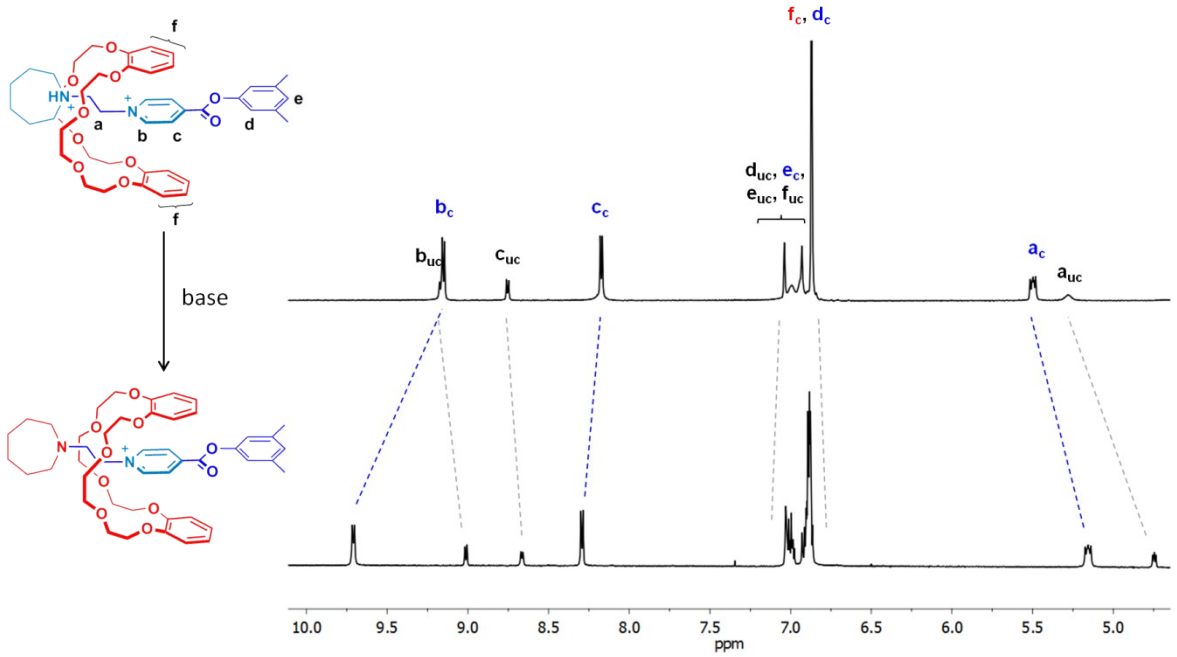

Fig. S5.14. Partial ^{1}H NMR spectra (500 MHz, CD_3NO_2, 20 °C, 10^{-2} M) of an equimolar solution of [**1-Aze·H**][PF_6]$_2$ and **DB24C8**: (top) when the equilibrium had been reached, (bottom) the same NMR sample after the addition of one equivalent of potassium *tert*-butoxide; showing that the deprotonated complex [**1-Aze**⊂DB24C8][PF_6] does not dissociate in their individual components. The system was monitored for almost thirty days. Lines highlight the changes on the resonances upon base addition (uc = uncomplexed; c = complexed).

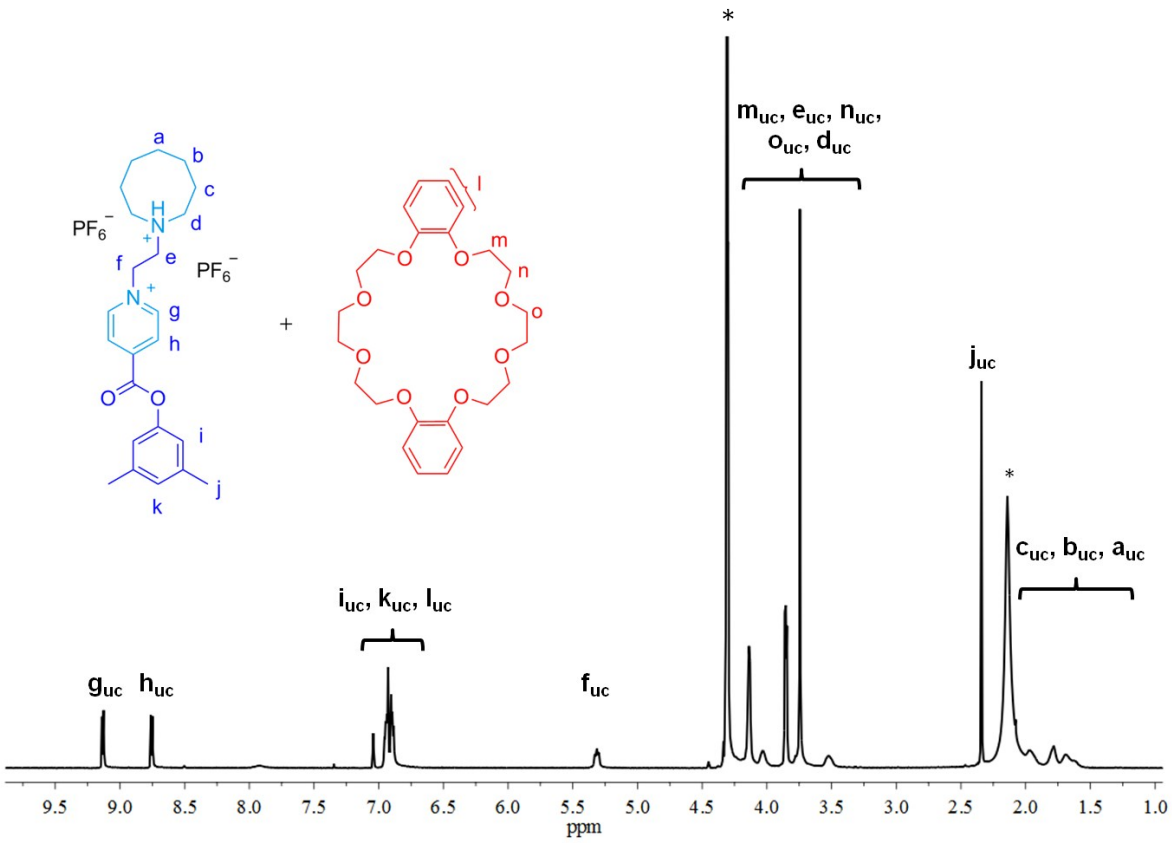

Fig. S5.15. ^{1}H NMR spectrum of an equimolar solution of [**1-Azo·H**][PF_6]$_2$ and **DB24C8** (500 MHz, CD_3NO_2, 20 °C, 10^{-2} M). There was no evidence of association from the individual components after twenty days (uc = uncomplexed; * = residual solvent).

Table S5.1. ^{1}H NMR chemical shifts for complexes.

Complex	Solvent	*ortho*-N^+ δ(Δδ)	*meta*-N^+ δ(Δδ)	CH_2-pyridine δ(Δδ)	CH_2-amine δ(Δδ)
[**1-Pi**·**H**⊂DB24C8]$^{2+}$	Acetone-d_6	9.49 (-0.04)	8.43 (-0.47)	[a]	4.53 (+0.21[b])
	Acetonitrile-d_3	9.12 (+0.14)	8.10 (-0.56)	5.32 (+0.31)	[a]
	Nitrometane-d_3	9.10 (-0.02)	8.14 (-0.62)	5.53 (+0.23)	4.55 (+0.54[b])
[**1-Tm**·**H**⊂DB24C8]$^{2+}$	Acetone-d_6	9.48 (-0.04)	8.41 (-0.49)	[a]	4.63 (+0.19)
	Acetonitrile-d_3	9.13 (+0.16)	8.09 (-0.57)	5.32 (+0.32)	4.27 (+0.62[b])
	Nitrometane-d_3	9.12 (-0.01)	8.16 (-0.59)	5.53 (+0.08)	4.61 (+0.57[b])
[**1-Mp**·**H**⊂DB24C8]$^{2+}$	Acetone-d_6	9.53 (-0.04)	8.33 (-0.54)	5.70 (+0.13)	4.52 (+0.35[b])
	Acetonitrile-d_3	9.15 (+0.10)	8.04 (-0.60)	5.37 (+0.29)	4.28 (+0.63[b])
	Nitrometane-d_3	9.17 (-0.14)	8.13 (-0.63)	5.53 (+0.04)	4.60 (+0.60[b])
[**1-Aze**·**H**⊂DB24C8]$^{2+}$	Acetone-d_6	9.57 (+0.04)	8.51 (-0.39)	[a]	[a]
	Acetonitrile-d_3	9.20 (+0.22)	8.15 (-0.51)	5.33 (+0.34)	[a]
	Nitrometane-d_3	9.14 (-0.04)	8.18 (-0.60)	5.52 (+0.16)	4.61 (+0.55[b])
[**3**⊂DB24C8]$^{1+}$	Acetone-d_6	9.99 (+0.54)	8.46 (-0.31)	5.11 (-0.21)	3.50 (-0.06)
	Acetonitrile-d_3	9.77 (+1.02)	8.15 (-0.34)	5.03 (+0.14)	[a]
	Nitrometane-d_3	9.90 (+1.06)	8.22 (-0.39)	5.14 (+0.09)	[a]

The data were obtained from ^{1}H NMR spectra of 1 : 1 (host : guest) mixtures (20 °C, 10^{-2} M). [a] Overlapped signal. [b] The $\Delta\delta$ was calculated from the δ of the CH_2-protons for the linear component in absence of **DB24C8**.

6. Thermodynamic data for the complexes

Table S6.1. Thermodynamic data for the synthesis[a] of complexes in CD_3NO_2 at 20 °C.

Complex	K_a (M^{-1})[b]	$\Delta G°$ (kJ mol^{-1})[c]
[**1-Pi**·**H**⊂DB24C8]$^{2+}$	1.8 (±0.1) × 10^3	-18.3 (±0.3)
[**1-Pi**⊂DB24C8]$^{1+}$	0.7 (±0.03) × 10^1	-4.8 (±0.2)
[**1-Tm**·**H**⊂DB24C8]$^{2+}$	1.9 (±0.1) × 10^3	-18.4 (±0.2)
[**1-Mp**·**H**⊂DB24C8]$^{2+}$	3.8 (±0.1) × 10^2	-14.5 (±0.1)
[**1-Aze**·**H**⊂DB24C8]$^{2+}$	1.6 (±0.2) × 10^3 [d]	-18.0 (±0.3)
[**3**⊂DB24C8]$^{1+}$	0.5 (±0.06) × 10^1	-4.1 (±0.3)

[a] The reactions were followed with ^{1}H NMR spectroscopy by monitoring the changes in the relative intensities for the signals associated with the probe protons in the complexed and uncomplexed guests. [b] The K_a values were obtained from single-point measurements of the concentrations of the complexed and uncomplexed guests, in the appropriate ^{1}H NMR spectrum, by using the expression K_a = [complex]/[guest][host]. [c] The free energies of association ($\Delta G°$) were calculated using the relationship $\Delta G° = - RT \ln K_a$; R corresponds to the gas constant. [d] The equilibrium was reached 14 days after mixing. Probe protons: *meta*-N^+ (pyridinium).

7. van't Hoff plots

Variable temperature ^{1}H NMR experiments were used to determinate the thermodynamic variables $\Delta H°$ and $\Delta S°$ for those adducts which undergoing slow interchange on the NMR time scale when the time needed to reach equilibrium was less than 48h. van't Hoff plots were obtained for each system.

Table S7.1. Thermodynamic parameters calculated from the variable temperature ^{1}H NMR experiments.

T (°C)	$[3]^{1+}$ + DB24C8	$[1\text{-Pi}\cdot H]^{2+}$ + DB24C8	$[1\text{-Tm}\cdot H]^{2+}$ + DB24C8	$[1\text{-Mp}\cdot H]^{2+}$ + DB24C8
		K_a (M^{-1})		
-20	34	-[b]	-[b]	3399
-10	21	-[b]	-[b]	1588
0	13	10023[c]	-[b]	1017
10	7	3608[d]	-[b]	545
20	5	1864	2000	358
30	3	1289	1403	257
40	2	758	789	184
50	1	505	512	134
60	-[a]	314	308	101
70	-[a]	182	211	81
80	-[a]	118	117	55
90	-[a]	74	75	31
		$\Delta H°$ (kJmol^{-1})		
	-32.7	-42.4	-42.0	-30.1
		$\Delta S°$ (Jmol^{-1}K^{-1})		
	-99.1	-80.4	-78.8	-52.7

The data were obtained from the equimolar mixtures ^{1}H NMR spectra ([guest] = [host] = 10^{-2}M, CD_3NO_2). [a] No evidence of complex formation. [b] The K_a value was not measured. The time needed to reach equilibrium was approximately 36[c] and 19[d] hours.

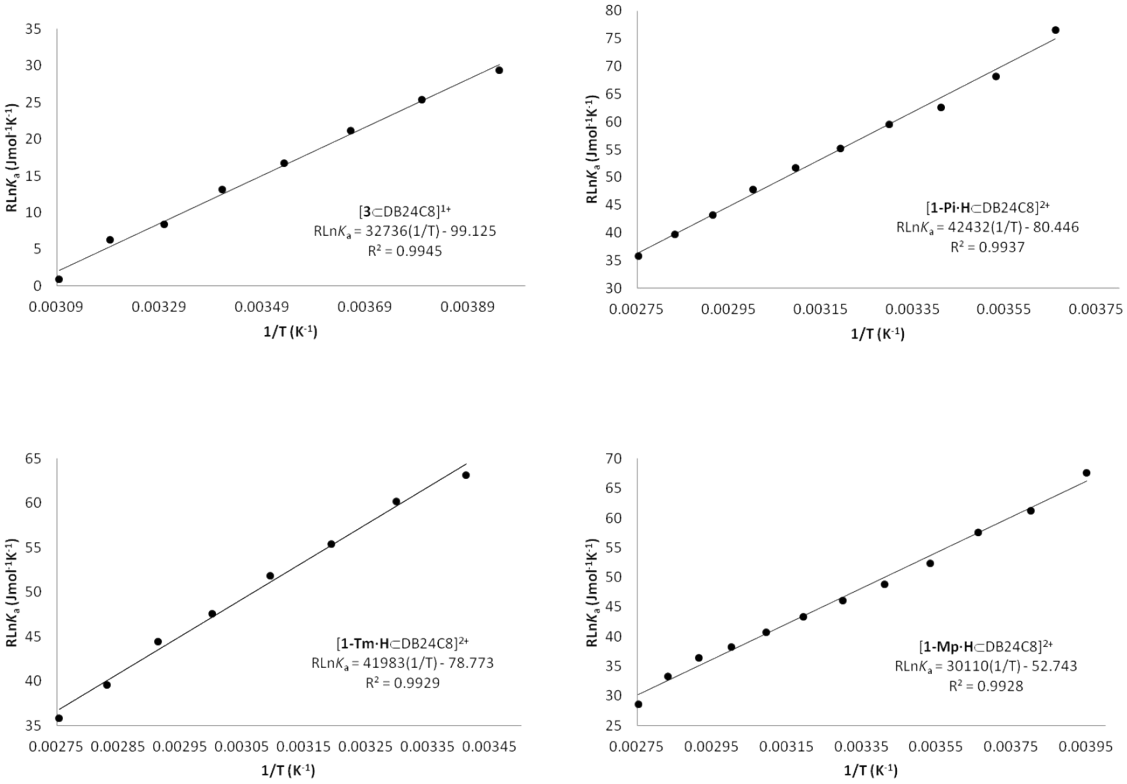

Fig. S7.1 van't Hoff plots. The equation and the linear correlation coefficient for each system are shown.

8. Rate constant determinations

Second order rate constants. An equimolar mixture of **DB24C8** (*M*) and the appropriate dumbbell salt (*D*) was dissolved in CD_3NO_2 to adjust the concentration of the species to 10^{-2} M. Only in the case of the [**1-Pi·H**⊂DB24C8][PF_6]$_2$ complex the sample was placed in a NMR spectrometer where the ^{1}H NMR spectra were recorded at 20 °C, at regular time intervals, until the equilibrium was attained. For the complex [**1-Aze·H**⊂DB24C8][PF_6]$_2$, it was not practicable to leave the sample in the NMR spectrometer; the reaction had to be carried out in a covered NMR tube which were heated in a thermostatic bath at 20 °C. Samples were removed at regular time intervals and their ^{1}H NMR spectra recorded.

By evaluating the relative intensities of the probe protons (*meta*-N^+), the concentrations of the free and complexed dumbbell at time, *t*, could be calculated from each spectrum. The second-order rate constants for the slippage processes (k_{on}) were calculated employing equation 1, from the nonlinear curve fitting of the plot of the complex concentration, $[C]_t$, against *t* (see Figure S8.1).

$$[C]_t = \frac{[D]_0^2[C]_e e^{\left(\frac{k_{on}t\left([D]_0^2 - [C]_e^2\right)}{[C]_e}\right)} - [D]_0^2[C]_e}{[D]_0^2 e^{\left(\frac{k_{on}t\left([D]_0^2 - [C]_e^2\right)}{[C]_e}\right)} - [C]_e^2} \quad (1)$$

Equation 1 was derived from the integrated rate equation (1.1)[5] for a reaction between two reactants (*D* and *M*) and a solitary product (*C*). In the equations, (i) $[D]_0$, (ii) $[C]_t$, and (iii) $[C]_e$ correspond to the initial dumbbell concentration (i), and the concentration of the complex after a certain time (ii) and at equilibrium (iii), respectively. Equation 1.1 may then be rearranged to provide equation 1.

$$k_{on}t = \left(\frac{[C]_e}{[D]_0^2 - [C]_e^2}\right) ln\left(\frac{[C]_e\left([D]_0^2 - [C]_e[C]_t\right)}{[D]_0^2\left([C]_e - [C]_t\right)}\right) \quad (1.1)$$

When the equilibrium between reactants and the complex is reached, the rates of slippage and extrusion become identical. Equation 1.2 can be used to calculate the rate constants for the extrusion processes, k_{off}, from the K_a and k_{on} values.

$$K_a = \frac{k_{on}}{k_{off}} \quad (1.2)$$

First order rate constant. An equimolar mixture of **DB24C8** and [**1-Pi·H**][PF_6]$_2$ was dissolved in CD_3NO_2 to adjust the concentration of the species to 10^{-2} M. Once the system had reached the equilibrium, one equivalent of potassium *tert*-butoxide (1.0M in *tert*-butanol) was added to deprotonate the complex and the corresponding free dumbbell. The sample was immediately placed in a NMR spectrometer where the ^{1}H NMR spectra were recorded at 20 °C, at regular time intervals, until the equilibrium was attained.

By evaluating the relative intensities of the probe protons specified, the concentrations of the free and complexed dumbbell at time, *t*, could be calculated from each spectrum. The first-order rate constant for the extrusion process (k_{off}) was calculated employing equation 2, from the nonlinear curve fitting of the plot of the free deprotonated dumbbell concentration, $[D']_t$, against *t* (see Figure S8.1).

$$[D']_t = \frac{[C]_0[D']_e\left[e^{\left(\frac{k_{off}t\left(2[C]_0 - [D']_e\right)}{[D']_e}\right)} - 1\right]}{[C]_0\left[1 + e^{\left(\frac{k_{off}t\left(2[C]_0 - [D']_e\right)}{[D']_e}\right)}\right] - [D']_e} \tag{2}$$

Equation 2 was derived from the integrated rate equation (2.1)[5] for a reaction between one reactant (*C*) that generates two products with the same concentration (*D'* and *M*). In the equations, (i) $[C]_0$, (ii) $[D']_t$, and (iii) $[D']_e$ correspond to the initial complex concentration (i), and the concentration of the free deprotonated dumbbell [**1-Pi**]$^{1+}$ after a certain time (ii) and at equilibrium (iii), respectively. Equation 2.1 may then be rearranged to provide equation 2.

$$k_{off}t = \left(\frac{[D']_e}{2[C]_0 - [D']_e}\right)ln\left(\frac{[C]_0[D']_e + [D']_t\left([C]_0 - [D']_e\right)}{[C]_0\left([D']_e - [D']_t\right)}\right) \tag{2.1}$$

When the equilibrium between the complex and the products is reached, the rates of slippage and extrusion become identical. Equation 1.2 can be used to calculate the rate constant for the slippage process, k_{on}, from the K_a and k_{off} values.

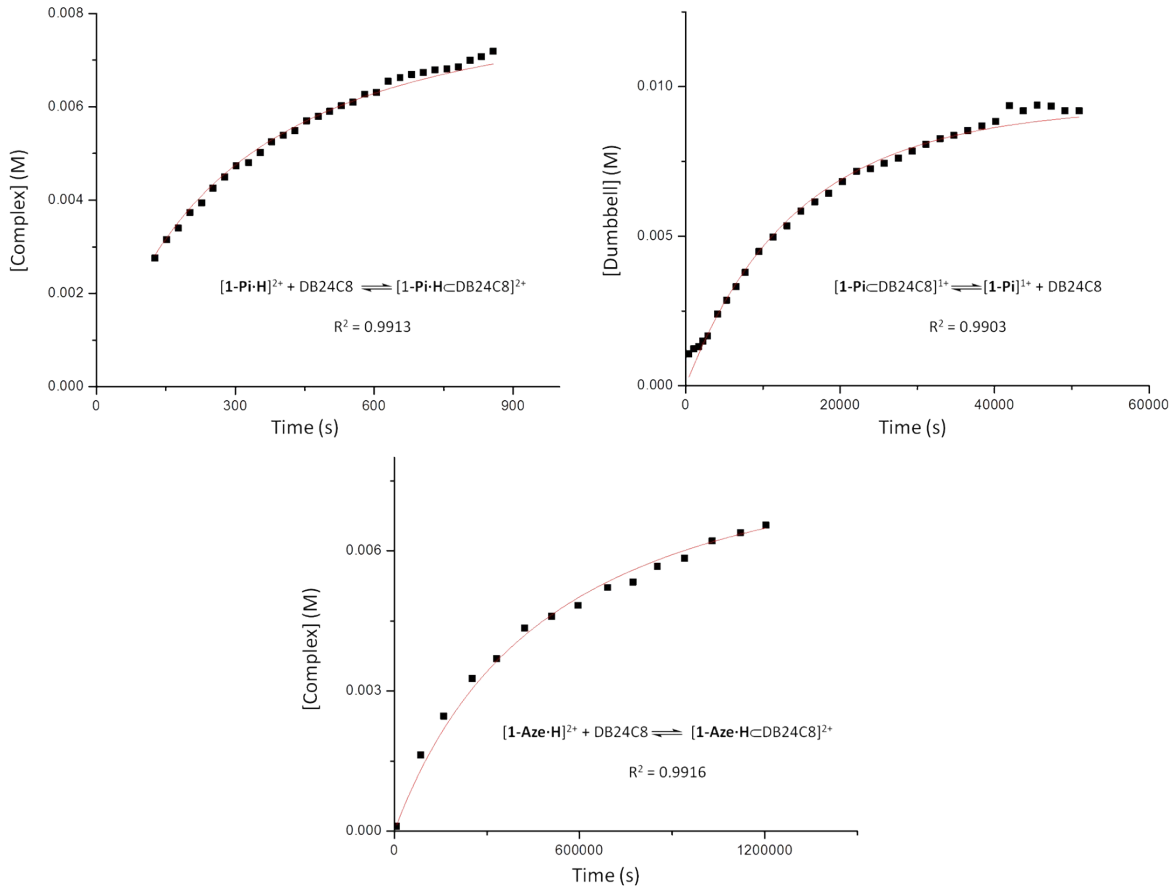

Fig. S8.1 Nonlinear curve fitting. The correlation coefficient for each system is shown.

Curve fitting. The quality of the nonlinear curve fitting of the experimental data using equations 1 or 2 was evaluated using the "Chi-square" statistical index (χ^2). Ideally, χ^2 is equal to zero for a perfect fit. In the Table S8.1, we observed low χ^2 values for our kinetic experiments, indicating the high quality of non linear curve fitting.

Table S8.1. Calculated χ^2 values for the nonlinear curve fitting of the kinetic data for the slippage or extrusion processes.

Complex	Rate constant calculated	χ^2
[**1-Pi·H**⊂DB24C8][PF_6]$_2$	k_{on} = 3.14 (±0.03) ×10^{-1} M^{-1}s^{-1}	1.42 x 10^{-8}
[**1-Pi**⊂DB24C8][PF_6]	k_{off} = 8.60 (±0.18) ×10^{-5} s^{-1}	7.85 x 10^{-8}
[**1-Aze·H**⊂DB24C8][PF_6]$_2$	k_{on} = 1.77 (±0.04) ×10^{-4} M^{-1}s^{-1}	2.95 x 10^{-8}

9. References

(1) L. M. Jackman, M. M. Petrei and B. D. Smith, *J. Am. Chem. Soc.*, 1991, **113**, 3451-3458.

(2) R. Lakhan and O. P. Singh, *Arch. Pharm.*, 1985, **318**, 228-238; L. H. Amundsen and K. W. Krantz, *J. Am. Chem. Soc.*, 1941, **63**, 305-307; F. Cortese, *J. Am. Chem. Soc.*, 1936, **58**, 191-192.

(3) T. A. Blizzard *et al.*, *Bioorg. Med. Chem. Lett.*, 2004, **14**, 3865-3868.

(4) C. Chiappe, C. S. Pomelli and S. Rajamani, *J. Phys. Chem. B*, 2011, **115**, 9653-9661.

(5) K. J. Laidler, *Chemical Kinetics*, McGraw-Hill, 2nd ed., USA, 1965, pp. 19-21.